

Differentially Private Range Queries with Correlated Input Perturbation

Prathamesh Dharangutte
Rutgers University
prathamesh.d@rutgers.edu

Jie Gao
Rutgers University
jg1555@rutgers.edu

Ruobin Gong
Rutgers University
ruobin.gong@rutgers.edu

Guanyang Wang
Rutgers University
guanyang.wang@rutgers.edu

Abstract

This work proposes a class of locally differentially private mechanisms for linear queries, in particular range queries, that leverages correlated input perturbation to simultaneously achieve unbiasedness, consistency, statistical transparency, and control over utility requirements in terms of accuracy targets expressed either in certain query margins or as implied by the hierarchical database structure. The proposed Cascade Sampling algorithm instantiates the mechanism exactly and efficiently. Our bounds show that we obtain near-optimal utility while being empirically competitive against output perturbation methods.

1 Introduction

We construct a class of locally differentially private mechanisms for linear queries, including range queries, representable as a multiplicative operation of a pre-specified workload matrix and a confidential database.

The proposed design leverages correlated input perturbation to simultaneously satisfy the following crucial properties:

Unbiasedness: The sanitized output exhibits no bias with respect to the ground truth;

Consistency (internal): The sanitized output may plausibly be viewed as having been queried directly from an input database without modification;

Statistical transparency: The probabilistic description of the sanitized output is analytically tractable to enable reliable downstream statistical inferences;

Utility control: The mechanism accommodates custom, externally specified utility requirements, expressed in terms of accuracy targets in certain query margins or as implied by the hierarchical database structure;

Efficient implementation: The proposed algorithm is exact and simple to implement, with no need for approximate simulation (including Markov chain Monte Carlo) nor optimization-based post-processing.

The curation of official statistics vividly illustrates the need and the challenge to simultaneously satisfy the above desiderata. As an example, the 2020 U.S. Decennial Census provide multi-resolutional tabular data products that follow a hierarchical system termed the “spine” [Abowd et al. \(2022\)](#), which orders from top to bottom geographic entities (states, counties, tracts, block groups, and blocks), with higher-level geographies partitioned by the lower-level ones. Population tabulations across the geographic resolutions are subject to numerous complex utility requirements. For example, state-level populations must be exactly reported per their constitutional purpose for reapportionment – an “invariant” requirement akin to *external* consistency; see [Gao et al. \(2022\)](#); [Dharangutte et al. \(2023\)](#). Tabulations at intermediate geographies must meet accuracy targets according to the relevant operational standards [U.S. Census Bureau \(2022\)](#), as does certain “off-spine” geographies (e.g. voting districts). Consistency both along and across the spine ensures logical stability in downstream numerical summaries. Furthermore, unbiasedness and statistical transparency influence both the quality and usability of the data product [Fioretto and Van Hentenryck \(2019\)](#); [Gong \(2022\)](#).

To the best of our knowledge, the proposed mechanism is the first in the literature of differentially private linear queries to satisfy all five desirable properties at once. To achieve this, the proposal adopts a variant of local differential privacy with correlated noises, which reduces error magnitude and offers fine control over utility. Local DP has many advantages thanks to its straightforward privacy error distribution, giving rise to unbiased, consistent, and transparent mechanisms that are practically easy to implement, particularly in distributed environments. However, a major limitation to local DP is that the noise magnitude in aggregated queries can become unacceptably large — e.g., the sum of n i.i.d. Gaussian variables has a variance of $\Theta(n)$ — an issue exacerbated in composite or multidimensional data products, severely hindering query usability.

Our proposal addresses the “runaway error magnitude” issue of local DP while harnessing its many strengths. The proposed mechanism carefully couples the local privacy noises to allow queries at different hierarchical levels to conform to a *uniform* accuracy standard while achieving *near-optimal* overall utility objectives, both theoretically and empirically. We show for 1D range queries, the proposed mechanism achieves optimal mean square error and near-optimal worst-case and expected worst-case errors when compared to prevailing (ϵ, δ) -DP mechanisms that do not meet all of consistency, transparency, and utility control requirements. The special error correlation structure supports a linear time efficient implementation called the Cascade Sampling algorithm. Importantly, the fine control over data utility at different levels of geography is inherent to the design of the proposed mechanism, rather than reliant on optimization-based post-processing which may destroy transparency and render unpredictable accuracy behavior. Our proposal can be generalized to other hierarchical and multidimensional linear query settings.

2 Problem Formulation

2.1 Problem Definition

Given a confidential data vector \mathbf{x} of dimension n , and a workload matrix \mathbf{W} of dimension $p \times n$, we would like to report a (possibly) noisy version of the query answer $\mathbf{W}\mathbf{x}$ while preserving the privacy of individual data elements in \mathbf{x} . \mathbf{W} is an incidence matrix with rows corresponding to queries and columns corresponding to data elements. Specifically, we consider an (ϵ, δ) -differentially private mechanism $\mathcal{W}_{\epsilon, \delta}$ which satisfies for any two neighboring databases \mathbf{x}, \mathbf{x}' , $\|\mathbf{x} - \mathbf{x}'\|_1 \leq 1$,

$$\mathbb{P}[\mathcal{W}_{\epsilon, \delta}(\mathbf{x}) \in D] \leq e^\epsilon \cdot \mathbb{P}[\mathcal{W}_{\epsilon, \delta}(\mathbf{x}') \in D] + \delta,$$

where D is any set of output values.

The linear query framework models many scenarios in practice. Three are particularly relevant to this work. *Predicate counting queries* report the number of database rows that satisfy the given predicate q , which are encoded into the rows of the workload matrix \mathbf{W} . *Range queries* report the sum of elements (or coordinates; x_i) that fall inside a given range, such as a time interval $[\ell, r]$ (e.g. streaming data) or a two-dimensional geographic area, with the structure of the range reflected in \mathbf{W} . *Contingency tables* are multidimensional histograms of entities satisfying certain composite attributes in a database. They can be regarded as a special type of high-dimensional range query, and are used extensively by statistical agencies for data processing and dissemination.

2.2 Desirable Properties of DP Mechanisms

Proposition 2.1. *A mechanism $\mathcal{W}_{\epsilon, \delta}$ is unbiased if*

$$\mathbb{E}(\mathcal{W}_{\epsilon, \delta}(\mathbf{x})) = \mathbf{W}\mathbf{x},$$

where the expectation is taken over the randomness of $\mathcal{W}_{\epsilon, \delta}$.

That is, unbiasedness requires a privacy mechanism to refrain from introducing systematic bias to the data output.

Proposition 2.2 (Gong (2022), Def. 3). *A privacy mechanism \mathcal{W} is statistically transparent if the conditional distribution of its output given the input,*

$$p_\xi(\mathcal{W} = w \mid \mathbf{x} = x),$$

is analytically available up to p and ξ , where ξ is the parameter (tuning and auxiliary) for p .

Statistical transparency is not frequently discussed in the literature of private mechanism design, but it is crucial if the sanitized output is subject to further data analysis. Knowledge about the probabilistic relationship between the observed query and the confidential data provides the basis for valid statistical uncertainty quantification [Gong \(2022\)](#).

Proposition 2.3. *A mechanism $\mathcal{W}_{\varepsilon,\delta}$ operating on the data vector \mathbf{x} is internally consistent if with probability one (over the randomness of $\mathcal{W}_{\varepsilon,\delta}$) there exists a vector \mathbf{x}' such that $\mathcal{W}_{\varepsilon,\delta}(\mathbf{x}) = \mathbf{W}\mathbf{x}'$.*

First defined for contingency tables and generalizable to any data output, consistency requires that the sanitized query may be viewed as a legitimate output of the intended query applied to a potential input database [Barak et al. \(2007\)](#); [Hay et al. \(2010\)](#); [Chan et al. \(2011\)](#).

Consistency is particularly important if the sanitized output enters directly into downstream decisions, for which it is expected to be free of internal logical conflicts.

Remark 2.4. For linear queries, consistency requires the sanitized output to be in the column space of \mathbf{W} . Any implied logical relationship embodied in \mathbf{W} (e.g. if one range is the union of two other disjoint ranges) would be mirrored in $\mathcal{W}_{\varepsilon,\delta}$. Additive mechanisms of the form $\mathbf{W}\mathbf{x} + \mathbf{e}$ may not enjoy consistency because the error \mathbf{e} , unless specifically designed, is not in the column space of \mathbf{W} with probability one. The same is true for exponential mechanisms unless their range is intentionally controlled [Seeman et al. \(2022\)](#).

Note that existing designs predominantly achieve consistency via optimization-based post-processing, which may enhance the overall accuracy of the mechanism at the price of statistical transparency. [Section 2.3](#) and [Appendix A](#) discuss these issues in more detail.

The property of *utility control* has been scarcely discussed in the literature, as the focus has been predominantly placed on the assessment of overall utility (such as average or worst-case), rather than the control over custom specified or fine-grained utility targets. We defer the discussion on utility control and *efficient implementation* to [Section 3](#) and [4](#) when we describe the proposed mechanism design.

2.3 A brief review of related literature

This section provides an abridged review of existing DP mechanisms for linear queries. Due to space constraints, we center our comments on [Table 1](#) and defer an extended literature review to [Appendix A](#).

Local DP utilizes *input perturbation* by altering every data entry in a controlled manner, and directly reporting linear queries from the perturbed data. Local DP mechanisms typically support unbiasedness, logical consistency, and statistical transparency, and are practically implementable particularly in distributed environments. However, local DP cannot support fine utility control and typically results in poor data utility, an issue that becomes worse when the query range contains a large number of data elements [Chan et al. \(2011\)](#). For this reason, input perturbation methods have been largely under-utilized in practice.

As a quintessential *output perturbation* method, *Gaussian mechanisms* add to the query output centered Gaussian noise with variance tailored to its sensitivity [Dinur and Nissim \(2003\)](#); [Dwork and Nissim \(2004\)](#); [Dwork et al. \(2006\)](#); [Hardt and Talwar \(2010\)](#); [Nikolov et al. \(2013\)](#), which for linear queries is the largest norm of the columns of workload matrix \mathbf{W} . Gaussian mechanisms are unbiased and statistically transparent, but are not flexible in utility control because the accuracy of the entire output query is dictated by \mathbf{W} . They are also not generally consistent for the reason discussed in [Remark 2.4](#).

Table 1: A comparison of properties among existing design choices for differentially private linear queries.

	unbiasedness	consistency (internal)	statistical transparency	utility control
Local DP	Yes	Yes	High	No
Gaussian mechanisms	Yes	No	High	No
Matrix mechanisms, e.g. Li et al. (2015)	Yes	No	High	No
Mechanisms with post-processing	Generally no	Yes	Low	No
TopDown Algorithm Abowd et al. (2022)	No	Yes	Low	Yes
Subspace DP Gao et al. (2022) ; Dharangutte et al. (2023)	Yes	No	High	Yes

The *matrix mechanism* Li et al. (2015) is a workload-dependent mechanism. It finds a privileged factorization, $\mathbf{W} = RA$, and infuses Gaussian noise to the intermediate result Ah , with h being the histogram vector. Choice in the factorization allows for the attainment of near optimal utility.

The matrix mechanism is unbiased and statistically transparent, but fails consistency and utility control for similar reasons as the Gaussian mechanisms.

Consistency may be enforced by *post-processing* if a mechanism does not already respect it, such as by projection into a designated subspace Li et al. (2015) or other optimization-based transformations. Post-processing does not generally maintain unbiasedness, though certain projections performed on additive mechanisms maintain unbiasedness if no inequality constraints are present, e.g. Barak et al. (2007); Hay et al. (2010). Moreover, except in special cases for which an analytical description is available, e.g. Hay et al. (2010), post-processing induces intractable probabilistic dependency between the query and the input database, e.g. Hardt et al. (2012), deteriorating statistical transparency.

The Census Bureau’s *TopDown algorithm* Abowd et al. (2022) is a massive endeavor to meet the complex requirements discussed in Section 1. It consists of two phases: 1) the “measurement” phase injects additive discrete Gaussian noise Canonne et al. (2020) to confidential queries, thus enjoys the same properties as do the Gaussian mechanisms; 2) the “estimation” phase uses optimization-based post-processing to achieve consistency (internal and external) and complex utility control, but destroys unbiasedness and statistical transparency in the process Gong (2022).

Subspace DP mechanisms Gao et al. (2022); Dharangutte et al. (2023) are designed to impose external consistency on the data product without post-processing. External consistency is expressed through invariants, a collection of exact queries from the confidential database, and may be understood as a special utility requirement of zero privacy noise. Subspace DP mechanisms allow utility control over all invariant queries, unbiasedness, and statistical transparency, but do not generally guarantee internal consistency.

3 Correlated input perturbation mechanism

This section presents the design of the correlation matrix, an efficient algorithm to sample from this distribution, and the resulting privacy and utility guarantees. Extensions to general binary tree and 2-D data are discussed in Appendix B.

3.1 Correlation matrix

Let us consider a scenario where we have a set of n data points residing on a one-dimensional line. To simplify matters, we’ll assume that n is a power of 2, denoted as $n = 2^k$. Extensions will be discussed in Appendix B. Each data point will be represented by its binary form, utilizing k bits, as leaves of a perfect binary tree with height k . Nodes in the tree receive labels based on their position in a level-order traversal. For example, the root node is labeled as \emptyset , the nodes at depth 1 will have labels “0” and “1”, and so on. See Fig. 1 for an $k = 3$ example.

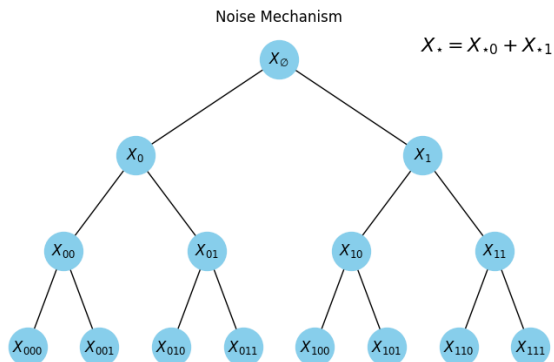


Figure 1: The mechanism assigns noises to every leaf node. For each internal node, the associated noise is the sum of its children.

Our objective is to allocate Gaussian random noises, denoted as $\{X_I\}_{I \in \{0,1\}^k}$, to every data point (i.e. leaf node). The noise imposed on each internal node is the sum of the noises of its two children. With our labeling convention, this relationship can be succinctly represented as $X_\star = X_{\star 0} + X_{\star 1}$, where \star stands for any binary sequence (including the empty one) with a length less than k .

If all the noises on the leaf nodes are independently and identically distributed (i.i.d.), we anticipate that the noise introduced at the root will have a Gaussian variance of $\Theta(n)$. However, by carefully coupling the Gaussian variables on the leaf nodes, we manage to establish uniform variance across all nodes in the binary tree. The structure of our correlation matrix is recursively defined below:

Definition 3.1. Take $\mathbf{C}_1 := \begin{pmatrix} 1 & -0.5 \\ -0.5 & 1 \end{pmatrix}$ and

$$\mathbf{C}_{i+1} := \begin{pmatrix} \mathbf{C}_i & -2^{-2i-1} \mathbf{J}_i \\ -2^{-2i-1} \mathbf{J}_i & \mathbf{C}_i \end{pmatrix}, \quad (1)$$

where \mathbf{J}_i is the all-one matrix of size $2^i \times 2^i$.

With each \mathbf{C}_i a square matrix of size $2^i \times 2^i$, we can now define our noise mechanism as follows.

Definition 3.2. For $n = 2^k$ data points identified by binary representation, our correlated noise mechanism is defined as $\text{Noise} = \sigma Z$. Here, $Z \sim \mathbb{N}(\mathbf{0}, \mathbf{C}_K)$, and the σ depends on a later-specified privacy budget. This mechanism applies to any private data vector \mathbf{x} , resulting in the output $\mathbf{x} + \text{Noise}$.

The structure outlined in [Definition 3.2](#) has a clear recursive pattern. One can split the 2^k data points into a left subtree, where labels begin with 0, and a right subtree, where labels begin with 1. The collection of points within each group mirrors a perfect binary tree of depth $k - 1$ with a covariance matrix of $\sigma^2 \mathbf{C}_{k-1}$. Points belonging to different groupings have a slightly negative correlation of -2^{-2k+1} . Similarly, points in the left subtree can be further divided based on those starting with 00 and those beginning with 01. Each of these smaller sub-groupings exhibits a covariance of \mathbf{C}_{k-2} , and any pair of points from these groups share a correlation of -2^{-2k+3} . This process can be recursively applied until each group is reduced to a single data point.

The next result shows that the variance of each internal node is the same as that of every leaf node.

Theorem 3.3. *Consider $n = 2^k$ data points identified by their binary representation as described earlier. Assuming the noise mechanism is defined as per [Definition 3.2](#), every node in the binary tree, including both leaf and internal nodes, has a marginal distribution of $\mathbb{N}(0, \sigma^2)$. This implies that each node shares an identical variance.*

Given that σ merely functions as a multiplicative constant within our privacy mechanism, our attention will now shift towards understanding some fundamental characteristics of \mathbf{C}_k , as listed below:

Proposition 3.4. *For a fixed positive integer k , the matrix \mathbf{C}_k exhibits the following properties:*

1. *The diagonal entries of \mathbf{C}_k are all 1.*
2. *Every off-diagonal element of \mathbf{C}_k is negative.*
3. *Summing over every column j for any row i , we have $\sum_j \mathbf{C}_k(i, j) = 2^{-k}$.*
4. *\mathbf{C}_k is a positive semi-definite (PSD) matrix.*

Proof of [Proposition 3.4](#). The initial two properties can be readily validated based on the matrix's definition. For the third property, it is evidently correct when $k = 1$. Assuming its correctness for $k = l$, when $k = l + 1$, we can deduce from [\(1\)](#) that

$$\sum_j \mathbf{C}_{l+1}(i, j) = \sum_j \mathbf{C}_l(i, j) + (-2^{-2l-1}) \times 2^l = 2^{-l} - 2^{-l-1} = 2^{-l-1} = 2^{-(l+1)}$$

as desired. The final property can be verified directly by applying the Gershgorin circle theorem based on the first three properties. \square

We now prove [Theorem 3.3](#).

Proof of [Theorem 3.3](#). Assuming, without a loss of generality, that $\sigma = 1$, we begin our proof by considering the case where $k = 1$. This essentially requires us to demonstrate that $X_\emptyset := X_0 + X_1$ has a unit variance. We have:

$$\text{Var}[X_\emptyset] = (1, 1) \cdot \mathbf{C}_1 \cdot (1, 1)^\top = 1 + 1 - 0.5 - 0.5 = 1$$

as desired. Now, let's assume the aforementioned result holds true for $k = l$. For $k = l + 1$, the formula (1), combined with our inductive assumption, confirms that every node in both the left and right subtrees maintains the same distribution $\mathbb{N}(0, 1)$. Consequently, our task narrows down to computing the variance for the root node X_\emptyset , which is given by:

$$\begin{aligned} \text{Var}[X_\emptyset] &= (1, 1, \dots, 1) \cdot \mathbf{C}_{l+1} \cdot (1, 1, \dots, 1)^\top \\ &= \sum_{i,j} \mathbf{C}_{l+1}(i, j) \\ &= \sum_i \sum_j \mathbf{C}_{l+1}(i, j) \\ &= \sum_i 2^{-(l+1)} = 1 \quad \text{by the [Item 3](#) in [Proposition 3.4](#).} \end{aligned}$$

This concludes our proof. □

3.2 Cascade Sampling algorithm

This section introduces an efficient algorithm for generating samples from our defined noise mechanism, specifically $\mathbb{N}(0, \sigma^2 \mathbf{C}_k)$ as defined in Formula (1). This method's computational cost is linear with the number of data points and outperforms standard Gaussian generation methods in scalability, as supported by theoretical and numerical evidence.

Assuming $\sigma = 1$ without loss of generality, the standard method for sampling an n -dimensional Gaussian $\mathbb{N}(\mu, \Sigma)$ involves Cholesky decomposition of the covariance matrix $\Sigma = LL^\top$, followed by transforming a standard Gaussian vector ($\mathbf{x} \sim \mathbb{N}(0, \mathbb{I}_n)$) using $L\mathbf{x} + \mu$. This process has a high computational cost, primarily due to the $O(n^3)$ expense of the Cholesky decomposition, with additional costs for sampling ($O(n)$) and transformation ($O(n^2)$).

Luckily, the recursive formula for covariance shown in (1) enables us to produce the required noise in $\Theta(n)$ time, where $n = 2^k$ represents the total number of data points. We call our method the Cascade Sampling algorithm ([Algorithm 1](#)) because it begins by sampling the noise at the highest level and propagates to the bottom most leaves, ensuring that the relationship $X_\star = X_{\star_0} + X_{\star_1}$ as well as the covariance matrix in (1) are both preserved.

Now we describe the detailed procedure of the noise mechanism. A simple yet crucial observation is the following: Given i.i.d. random variables $X, Y \sim \mathbb{N}(0, 1)$, define

$$X_0 = \frac{1}{2}X + \frac{\sqrt{3}}{2}Y, \quad X_1 = \frac{1}{2}X - \frac{\sqrt{3}}{2}Y. \tag{2}$$

Then X_0, X_1 are also $\mathbb{N}(0, 1)$, they sum up to X and has correlation -0.5 . [Fig. 2](#) provides a visual demonstration.

The construction allows for a recursive method, starting from the root and progressing to the leaves. Initially, a standard normal is sampled for the root's noise, then the noise for its direct descendants (depth 1 nodes) is determined using equation (2). This process is repeated, applying equation (2) for each subsequent level, to assign noise to all nodes. The complete process is outlined in [Algorithm 1](#).

Our next result shows the leaves have the covariance structure described in [Definition 3.2](#).

Proposition 3.5. *For any given positive integer k , the covariance matrix of the leaf noises produced by [Algorithm 1](#) is equal to $\sigma^2 \mathbf{C}_k$, where \mathbf{C}_k is defined in [Definition 3.1](#).*

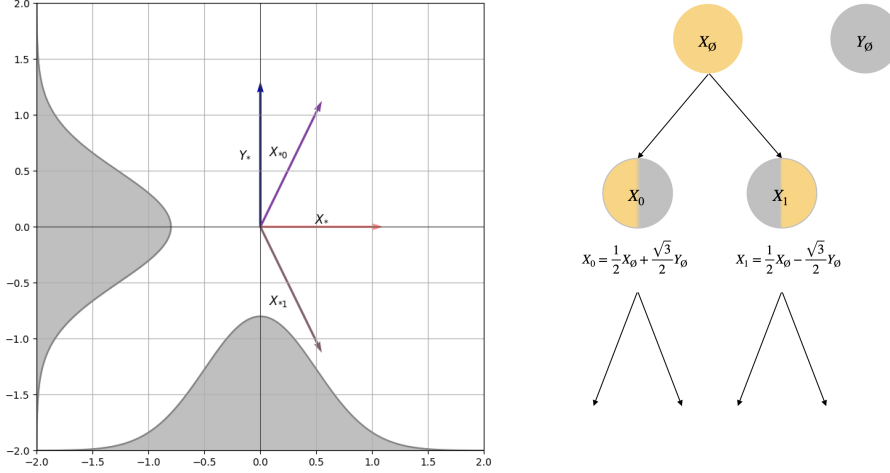


Figure 2: Left: Illustration of noise allocation to sibling nodes and their parent within a binary tree. Here X_* denotes the noise applied to a node labeled \star , and Y_* is another standard Gaussian independent of X_* . The noise values for the children nodes are $X_{\star 0} := X_*/2 + \sqrt{3}Y_*/2$ and $X_{\star 1} := X_*/2 - \sqrt{3}Y_*/2$. Right: Noise allocation on the top two levels of a binary tree.

Algorithm 1 Cascade Sampling Algorithm

Input: Depth of the binary tree k , variance σ^2 determined by the privacy budget.

Output: Noise values $\{X_I\}$ for all nodes $I \in \cup_{0 \leq i \leq k} \{0, 1\}^i$ in a binary tree.

for each node $\star \in \{0, 1\}^i$ at depth $0 \leq i \leq k - 1$ **do**

if $\star = \emptyset$ **then**

 Assign $X_{\emptyset} \sim \mathbb{N}(0, \sigma^2)$

end if

 Sample $Y_{\star} \sim \mathbb{N}(0, \sigma^2)$ independently

 Define the noise values for the children nodes of \star :

$X_{\star 0} := \frac{1}{2}X_{\star} + \frac{\sqrt{3}}{2}Y_{\star}$, $X_{\star 1} := \frac{1}{2}X_{\star} - \frac{\sqrt{3}}{2}Y_{\star}$

end for

Proof of Proposition 3.5. Without loss of generality, we assume $\sigma = 1$. We will prove by induction. When $k = 1$, it suffices to show the $\text{Var}(X_0) = \text{Var}(X_1) = 1$ and $\text{Cov}(X_0, X_1) = -0.5$. For the former, observe that

$$\text{Var}(X_0) = \text{Var}\left(\frac{1}{2}X_{\emptyset} + \frac{\sqrt{3}}{2}Y_{\emptyset}\right) = \left(\frac{1}{2}\right)^2 \text{Var}(X_{\emptyset}) + \left(\frac{\sqrt{3}}{2}\right)^2 \text{Var}(Y_{\emptyset}) = \frac{1}{4} + \frac{3}{4} = 1.$$

Similarly $\text{Var}(X_1) = 1$. For the covariance, we have

$$\text{Cov}(X_0, X_1) = \text{Cov}\left(\frac{1}{2}X_{\emptyset} + \frac{\sqrt{3}}{2}Y_{\emptyset}, \frac{1}{2}X_{\emptyset} - \frac{\sqrt{3}}{2}Y_{\emptyset}\right) = \left(\frac{1}{2}\right)^2 \text{Var}(X_{\emptyset}) - \left(\frac{\sqrt{3}}{2}\right)^2 \text{Var}(Y_{\emptyset}) = \frac{1}{4} - \frac{3}{4} = -0.5.$$

This concludes our proof for the $k = 1$ case. Assuming the result holds for $k = l$, we note that for $k = l + 1$, the nodes in the left subtree (labelled $X_{0\star}$) and the nodes in the right subtree (labelled $X_{1\star}$) each constitute a complete binary tree of depth l . Furthermore, the recursive nature of Algorithm 1 indicates that the following three sets of random variables are identically distributed:

$$\{X_{0\star}\}_{\star \in \cup_{0 \leq s \leq l} \{0, 1\}^s} \stackrel{d}{=} \{X_{1\star}\}_{\star \in \cup_{0 \leq s \leq l} \{0, 1\}^s} \stackrel{d}{=} \{\tilde{X}_{\star}\}_{\star \in \cup_{0 \leq s \leq l} \{0, 1\}^s}. \quad (3)$$

In this context, $\{X_{0\star}\}$ and $\{X_{1\star}\}$ represent the left and right subtrees generated by Algorithm 1 when $k = l + 1$, while $\{\tilde{X}_{\star}\}$ denotes an independent execution of Algorithm 1 with $k = l$. Employing equation (3)

and the inductive hypothesis for $k = l$ on the set $\{\tilde{X}_*\}_{*\in\bigcup_{0\leq s\leq l}\{0,1\}^s}$, we know that the covariance matrices restricted to the left and right subtrees are both equivalent to \mathbf{C}_l . Hence, the two $2^l \times 2^l$ diagonal blocks of \mathbf{C}_{l+1} are identical to \mathbf{C}_l .

To confirm that the entire covariance matrix is equal to \mathbf{C}_{l+1} as specified in (1), we must demonstrate that any leaf in the left subtree is correlated with any leaf in the right subtree by -2^{-2l-1} . Take any pair of indices $I, J \in \{0, 1\}^l$, and denote $\tilde{I} = (0, I_1, \dots, I_{l-1}) \in \{0, 1\}^l$ and $\tilde{J} = (1, J_1, \dots, J_{l-1}) \in \{0, 1\}^l$. **Algorithm 1** informs us that the noise at leaf X_{0I} is expressed as:

$$X_{0I} = \frac{1}{2}X_{\tilde{I}} + \frac{(-1)^{I_k}\sqrt{3}}{2}Y_{\tilde{I}},$$

and likewise for leaf X_{1J} :

$$X_{1J} = \frac{1}{2}X_{\tilde{J}} + \frac{(-1)^{J_k}\sqrt{3}}{2}Y_{\tilde{J}}.$$

Consequently:

$$\text{Cov}(X_{0I}, X_{1J}) = \left(\frac{1}{2}\right)^2 \text{Cov}(X_{\tilde{I}}, X_{\tilde{J}}), \quad (4)$$

since $Y_{\tilde{I}}$ is by construction independent of $X_{\tilde{J}}$ and $Y_{\tilde{J}}$ are independent of $X_{\tilde{I}}$. Given that $X_{\tilde{I}}$ and $X_{\tilde{J}}$ are leaf nodes on opposing sides of a binary tree of depth l , their covariance is -2^{-2k+1} by the inductive hypothesis. Inserting this into equation (4), we obtain:

$$\text{Cov}(X_{0I}, X_{1J}) = 2^{-2} \times -2^{-2k+1} = -2^{-2k-1}, \quad (5)$$

which completes the proof. \square

If one unit of cost is attributed to the sampling of a univariate normal variable and to each arithmetic operation (including addition or multiplication), it becomes clear that the cost of **Algorithm 1** is linear in the total number of data points, dramatically improving the $O(n^3)$ cost of the standard sampling algorithm using Cholesky decomposition.

Proposition 3.6. *The execution of **Algorithm 1** with a given input depth k incurs a cost of $\Theta(2^k)$. Thus, the algorithm's cost is proportional to $\Theta(n)$, where $n = 2^k$ represents the total count of data points (leaf nodes).*

Finally, combining **Proposition 3.5** and **Theorem 3.3** immediately shows that the noises on every node generated by **Algorithm 1** have the same distribution $\mathbb{N}(0, \sigma^2)$. More importantly, our correlation matrix \mathbf{C}_k has many more interesting properties that are central to privacy and utility analysis. The determination of σ^2 and further properties of \mathbf{C}_k will be explored in the forthcoming sections.

3.3 Privacy property

We now turn our focus to the privacy aspects of our algorithm, with a special emphasis on identifying the suitable level of noise. First, **Theorem 3.7** is applicable to Gaussian noise with any covariance matrix \mathbf{C} . This can be seen as an extension of the traditional Gaussian mechanism (e.g. Appendix A of **Dwork and Roth (2014)**) but for correlated noises. Then, **Theorem 3.8** is specifically tailored for the covariance matrix outlined in **Definition 3.1**.

Theorem 3.7. *Let $X \in \mathcal{X}^n$ be any dataset with $\|X - X'\|_2 \leq 1$ for neighboring X and X' and let $\mathcal{M}_\sigma(X) = X + \text{Noise}$ be the privacy mechanism, where $\text{Noise} \sim \mathbb{N}(\mathbf{0}, \sigma^2\mathbf{C})$ and \mathbf{C} is an arbitrary covariance matrix with dimension $n \times n$. Fix any $\varepsilon \in (0, 1]$ and $\delta \in (0, 1/2]$, the mechanism $\mathcal{M}_\sigma(\cdot)$ is (ε, δ) -DP for*

$$\sigma^2 \geq \frac{2\|\text{diag}(\mathbf{C}^{-1})\|_\infty \log(2/\delta)}{\varepsilon^2}$$

where $\|\text{diag}(\mathbf{C}^{-1})\|_\infty$ denotes the largest magnitude of the diagonal entries of \mathbf{C}^{-1} .

Proof of Theorem 3.7. To prove (ε, δ) -DP, we prove that with probability at least $1 - \delta$ the likelihood ratio between $\mathcal{M}_\sigma(X)$ and $\mathcal{M}_\sigma(X')$ is upper bounded by $\exp(\varepsilon)$, where X and X' are any two datasets that differ by at most one at only one entry. For now, we assume $X = X' + e_i$, where $e_i \in \mathcal{X}^n$ takes value 1 at the i -th coordinate, and 0 elsewhere. Let $s \in \mathbb{R}^n$ be any real vector, the logarithm of the likelihood ratio between $\mathcal{M}_\sigma(X)$ and $\mathcal{M}_\sigma(X')$ at point $X + s$ equals

$$\begin{aligned} \log \left(\frac{f_{\mathcal{M}_\sigma(X)}(X+s)}{f_{\mathcal{M}_\sigma(X')}(X+s)} \right) &= \log \left(\frac{\exp(-\frac{1}{2\sigma^2} s^\top \mathbf{C}^{-1} s)}{\exp(-\frac{1}{2\sigma^2} (s+e_i)^\top \mathbf{C}^{-1} (s+e_i))} \right) \\ &= -\frac{1}{2\sigma^2} \left(s^\top \mathbf{C}^{-1} s - (s+e_i)^\top \mathbf{C}^{-1} (s+e_i) \right) \\ &= \frac{1}{2\sigma^2} (\mathbf{C}^{-1})(i, i) + \frac{1}{\sigma^2} s^\top \mathbf{C}^{-1} e_i, \end{aligned}$$

In our noise mechanism, $s \sim \mathbb{N}(\mathbf{0}, \sigma^2 \mathbf{C})$. Therefore the above log-likelihood ratio is a one-dimensional Gaussian with mean

$$\frac{1}{2\sigma^2} (\mathbf{C}^{-1})(i, i),$$

and variance

$$\frac{1}{\sigma^2} e_i^\top \mathbf{C}^{-1} \mathbf{C} \mathbf{C}^{-1} e_i = \frac{1}{\sigma^2} \mathbf{C}^{-1}(i, i).$$

Let $Y \sim \mathbb{N}(0, 1)$ be a standard normal random variable, set $w = \mathbf{C}^{-1}(i, i)/\sigma^2$ for notational simplicity. It is then clear that $\sqrt{w}Y + w/2$ has the same distribution as $\log \left(\frac{f_{\mathcal{M}_\sigma(X)}(X+s)}{f_{\mathcal{M}_\sigma(X')}(X+s)} \right)$. Since $\sqrt{w}Y + w/2 \leq \varepsilon$ is equivalent to $Y \leq \varepsilon/\sqrt{w} - \sqrt{w}/2$, it suffices to find conditions on w such that $\mathbb{P}[|Y| \geq \varepsilon/\sqrt{w} - \sqrt{w}/2] \leq \delta$.

Applying the standard subgaussian tail bound on Y , we have

$$\mathbb{P}[Y > x] \leq 2 \exp(-x^2/2)$$

for every $x > 0$. Therefore it suffices to find w such that $\varepsilon/\sqrt{w} - \sqrt{w}/2 > 0$, and

$$\left(\frac{\varepsilon}{\sqrt{w}} - \frac{\sqrt{w}}{2} \right)^2 \geq \log \left(\frac{2}{\delta} \right).$$

Now we set $0 < w \leq \varepsilon^2/(2 \log(2/\delta))$, and check every w in this range satisfies the above two conditions. Firstly,

$$w \leq \varepsilon^2/(2 \log(2/\delta)) \leq \varepsilon^2/2 \log(4) \leq 2\varepsilon,$$

therefore $\varepsilon/\sqrt{w} - \sqrt{w}/2 > 0$. Secondly,

$$\frac{\varepsilon^2}{w} \geq 2 \log \left(\frac{2}{\delta} \right) \geq \log(2/\delta) + \log(4) > \log(2/\delta) + \varepsilon.$$

Therefore

$$\left(\frac{\varepsilon}{\sqrt{w}} - \frac{\sqrt{w}}{2} \right)^2 = \frac{\varepsilon^2}{w} - \varepsilon + \left(\frac{\sqrt{w}}{2} \right)^2 \geq \frac{\varepsilon^2}{w} - \varepsilon \geq \log(2/\delta),$$

as desired. This immediately translates to the noise bound

$$\sigma^2 \geq \frac{2(\mathbf{C}^{-1})(i, i) \log(2/\delta)}{\varepsilon^2}. \quad (6)$$

The above calculation still goes through when $X = X' - e_i$. Since the preceding argument must be valid for any i , taking the maximum of i from Equation (6) shows our mechanism $\mathcal{M}_\sigma(\cdot)$ is (ε, δ) -DP for

$$\sigma^2 \geq \frac{2 \|\text{diag}(\mathbf{C}^{-1})\|_\infty \log(2/\delta)}{\varepsilon^2}$$

□

Theorem 3.7 is broad in scope yet challenging to apply. It requires knowing the precision matrix (inverse of the covariance matrix), which is hard to estimate unless specifically designed. Luckily, our paper's noise model has a clearly defined inverse matrix, simplifying analysis and making the theorem more practical. Our dataset includes $n = 2^k$ points, using multivariate Gaussian noise with a covariance of $\sigma^2 \mathbf{C}_k$, as detailed in **Definition 3.1**. The key findings are presented in the following theorem.

Theorem 3.8. *Let $X \in \mathcal{X}^n$ be any dataset and let $\mathcal{M}_\sigma(X) = X + \text{Noise}$ be our privacy mechanism, where $\text{Noise} \sim \mathbb{N}(\mathbf{0}, \sigma^2 \mathbf{C}_k)$ with \mathbf{C}_k defined in **Definition 3.1**. Fix any $\varepsilon \in (0, 1]$ and $\delta \in (0, 1/2]$, our mechanism $\mathcal{M}_\sigma(\cdot)$ is (ε, δ) -DP for*

$$\sigma^2 \geq \left(\frac{2}{\varepsilon^2} + \frac{2 \log_2(n)}{3\varepsilon^2} \right) \log(2/\delta) = \Theta \left(\frac{\log(n) \log(2/\delta)}{\varepsilon^2} \right).$$

To establish **Theorem 3.8**, we need the following lemma.

Lemma 3.9. *For any positive integer j , \mathbf{C}_j^{-1} satisfies $\mathbf{C}_1^{-1} := \begin{pmatrix} 4/3 & 2/3 \\ 2/3 & 4/3 \end{pmatrix}$ and*

$$\mathbf{C}_j^{-1} = \begin{pmatrix} \mathbf{C}_{j-1}^{-1} + \frac{1}{3} J_{j-1} & \frac{2}{3} J_{j-1} \\ \frac{2}{3} J_{j-1} & \mathbf{C}_{j-1}^{-1} + \frac{1}{3} J_{j-1} \end{pmatrix},$$

where J_{j-1} is the all one matrix of size $2^{j-1} \times 2^{j-1}$.

Proof of Lemma 3.9. We prove a slightly stronger result. We show for every $k \geq 1$, the followings all hold:

1. $J_k \mathbf{C}_k = \mathbf{C}_k J_k = 2^{-k} J_k$
2. $J_k J_k = 2^k J_k$
3. $J_k \mathbf{C}_k^{-1} = 2^k J_k$
4. We have

$$\mathbf{C}_1^{-1} = \begin{pmatrix} 4/3 & 2/3 \\ 2/3 & 4/3 \end{pmatrix} \quad \mathbf{C}_k^{-1} = \begin{pmatrix} \mathbf{C}_{k-1}^{-1} + \frac{1}{3} J_{k-1} & \frac{2}{3} J_{k-1} \\ \frac{2}{3} J_{k-1} & \mathbf{C}_{k-1}^{-1} + \frac{1}{3} J_{k-1} \end{pmatrix}$$

We prove this by induction. All the four claims can be directly checked when $k = 1$. Assuming they are all satisfied when $k \leq K$, for $k = K + 1$, facts 1 and 2 can still be directly checked. To show fact 4, it suffices to show

$$\begin{pmatrix} A & B \\ C & D \end{pmatrix} := \begin{pmatrix} \mathbf{C}_K & -2^{-2K-1} J_K \\ -2^{-2K-1} J_K & \mathbf{C}_K \end{pmatrix} \cdot \begin{pmatrix} \mathbf{C}_K^{-1} + \frac{1}{3} J_K & \frac{2}{3} J_K \\ \frac{2}{3} J_K & \mathbf{C}_K^{-1} + \frac{1}{3} J_K \end{pmatrix} = I_{2^{K+1}}$$

We directly check this by multiplying the two 2×2 block matrices on the left hand side. The diagonal blocks are

$$A = D = I + \frac{1}{3} \mathbf{C}_K J_K - \frac{2}{3} \times 2^{-2K-1} J_K J_K = I + \frac{2^{-K}}{3} J_K - \frac{2^{-K}}{3} J_K = I$$

where the second to last equality follows from facts 1 and 2 of our induction hypothesis.

The off-diagonal blocks are:

$$B = D = \frac{2}{3} \mathbf{C}_K J_K - 2^{-2K-1} J_K \mathbf{C}_K^{-1} - \frac{2^{-2K-1}}{3} J_K J_K = \frac{4 \times 2^{-K-1}}{3} J_K - 2^{-K-1} J_K - \frac{2^{-K-1}}{3} J_K = 0$$

This concludes our induction for fact 4. Fact 3 is then immediate using fact 4 together with facts 1, 2 from the induction hypothesis. \square

The following corollary can be derived directly from **Lemma 3.9** by induction.

Corollary 3.10. *For any positive integer k , the diagonal entries of \mathbf{C}_j^{-1} all equal to $1 + j/3$.*

Theorem 3.8 is immediate by applying **Corollary 3.10** and **Theorem 3.7**.

Proof of Theorem 3.8. Based on **Corollary 3.10**, it becomes evident that the norm $\|\text{diag}(\mathbf{C}_k^{-1})\|_\infty$ equals $1 + k/3 = 1 + \log_2(n)/3$. Applying this into **Theorem 3.7** leads to our result. \square

3.4 Utility Analysis

We now evaluate the overall efficiency of our correlated input perturbation mechanism, $\mathcal{M}_\sigma(\mathbf{x}) = \mathbf{x} + \mathbb{N}(\mathbf{0}, \sigma^2 \mathbf{C}_k)$, for a dataset $\mathbf{x} \in \mathcal{X}^n$ where $n = 2^k$. Given a workload matrix \mathbf{W} , our mechanism operates by applying this matrix to the perturbed dataset, which we represent as $\mathcal{W}_\sigma(\mathbf{x}) := \mathbf{W}\mathcal{M}_\sigma(\mathbf{x})$. This design satisfies all the desired properties described in [Section 1](#). First, as an additive mechanism, \mathcal{W}_σ enjoys unbiasedness as the privacy noise \mathbf{e} has zero mean as guaranteed by design. Second, \mathcal{W}_σ maintains consistency as $\mathcal{M}_\sigma(\mathbf{x})$ could be viewed as a potential legitimate input. Furthermore, the additive construction of \mathcal{W}_σ , coupled with the public knowledge of the noise distribution as a correlated Gaussian makes \mathcal{W}_σ statistically transparent.

We outline various error metrics to quantify the discrepancy between $\mathcal{W}_\sigma(\mathbf{x})$ and $\mathbf{W}\mathbf{x}$. Since $\mathcal{W}_\sigma(\mathbf{x}) - \mathbf{W}\mathbf{x} = \mathbf{W} \cdot \text{Noise}$ where $\text{Noise} \sim \mathbb{N}(\mathbf{0}, \sigma^2 \mathbf{C}_k)$, we observe that the difference is a random vector that does not depend on the dataset \mathbf{x} . Some reasonable error metrics are as follows:

Definition 3.11 (Expected total squared error). The expected total squared error is defined as

$$\text{err}_{\mathbf{W},2}(\mathcal{W}_\sigma) := \sup_{\mathbf{x} \in \mathcal{X}^n} \mathbb{E}[\|\mathcal{W}_\sigma(\mathbf{x}) - \mathbf{W}\mathbf{x}\|_2^2] = \mathbb{E}_{\mathbf{s} \sim \mathbb{N}(\mathbf{0}, \sigma^2 \mathbf{C}_k)}[\|\mathbf{W}\mathbf{s}\|_2^2].$$

Definition 3.12 (Worst-case expected error). The worst-case expected error is defined as

$$\text{err}_{\mathbf{W}}^\infty(\mathcal{W}_\sigma) := \sup_{\mathbf{x} \in \mathcal{X}^n} \|\mathbb{E}[\|\mathcal{W}_\sigma(\mathbf{x}) - \mathbf{W}\mathbf{x}\|]\|_\infty = \|\mathbb{E}_{\mathbf{s} \sim \mathbb{N}(\mathbf{0}, \sigma^2 \mathbf{C}_k)}[\|\mathbf{W}\mathbf{s}\|]\|_\infty.$$

where $|v|$ applies to each component of v .

Definition 3.13 (Expected worst-case error). The expected worst-case error is defined as

$$\text{err}_{\mathbf{W},\infty}(\mathcal{W}_\sigma) := \sup_{\mathbf{x} \in \mathcal{X}^n} \mathbb{E}[\|\mathcal{W}_\sigma(\mathbf{x}) - \mathbf{W}\mathbf{x}\|_\infty] = \mathbb{E}_{\mathbf{s} \sim \mathbb{N}(\mathbf{0}, \sigma^2 \mathbf{C}_k)}[\|\mathbf{W}\mathbf{s}\|_\infty].$$

The difference between $\text{err}_{\mathbf{W}}^\infty$ and $\text{err}_{\mathbf{W},\infty}$ arises solely from the order in which \mathbb{E} and the ℓ_∞ norm are taken. We have the following relationship between these errors.

Proposition 3.14. For any given $\sigma > 0$ and query matrix \mathbf{W} of size $m \times n$, we have:

$$\sqrt{\text{err}_{\mathbf{W},2}(\mathcal{W}_\sigma)/m} \leq \text{err}_{\mathbf{W}}^\infty(\mathcal{W}_\sigma) \leq \text{err}_{\mathbf{W},\infty}(\mathcal{W}_\sigma). \quad (7)$$

Proof of Proposition 3.14. The first inequality directly follows from the fact that for any $\mathbf{v} \in \mathbb{R}^m$

$$\|\mathbf{v}\|_2^2 = \sum_{i=1}^m v_i^2 \leq m \|\mathbf{v}\|_\infty^2$$

The second inequality directly follows from the fact that for any random vector \mathbf{v} ,

$$\|\mathbb{E}[\mathbf{v}]\|_\infty \leq \mathbb{E}[\|\mathbf{v}\|_\infty]$$

□

The focus of our analysis is on two scenarios. The first is that \mathbf{W} represents all consecutive range queries. In this context, \mathbf{W} is a binary matrix of dimensions $\binom{n}{2} \times n$, with each row comprising a sequence of consecutive ones. The second is \mathbf{W} represents all ‘nodal’ queries, indicating that \mathbf{W} is a matrix of dimensions $(2n - 1) \times n$, designed to query the values associated with every node in our binary tree, as illustrated in [Fig. 1](#). We also recall the notations introduced in [Section 3.1](#), where $\{X_I\}_{I \in \{0,1\}^k}$ represents the Gaussian noise vector with a covariance matrix $\sigma^2 \mathbf{C}_k$.

3.4.1 Continuous range queries

When \mathbf{W} encompasses all continuous range queries, the related noise $\mathcal{W}_\sigma(\mathbf{x}) - \mathbf{W}$ forms a vector with a length of $\binom{n}{2} + n$. Each element in this vector represents a consecutive sum $\sum_{L=I}^{I+j} X_L$. Consequently, it's evident that each element is a univariate Gaussian with zero mean. The essential technical lemma below demonstrates that the maximum variance increases logarithmically with the number of data points.

Lemma 3.15. *Let $\{X_I\}_{I \in \{0,1\}^k} \sim \mathbb{N}(\mathbf{0}, \sigma^2 \mathbf{C}_k)$ with \mathbf{C}_k defined in [Definition 3.1](#). Then the maximum variance among all the consecutive sums satisfies:*

$$\max_{I \in \{0,1\}^k, j \leq 2^k - I} \text{Var}\left[\sum_{L=I}^{I+j} X_L\right] / \sigma^2 = \Theta(k) = \Theta(\log_2(n)).$$

Proof of [Lemma 3.15](#), upper bound. To prove the upper bound, our main idea is to argue that any fixed summation of the form $\sum_{L=I}^{I+k} X_L$ can be rewritten as a summation $\sum_{l=1}^T Y_l$, which satisfies the following properties:

- Each Y_l has variance σ^2
- Each pair of Y_i, Y_j has a non-positive correlation
- The term of summations $T = O(K)$.

Assuming all the three properties hold, putting these altogether shows

$$\text{Var}\left[\sum_{L=I}^{I+k} X_L\right] = \text{Var}\left[\sum_{l=1}^T Y_l\right] \leq \sum_{l=1}^T \text{Var}[Y_l] = \sigma^2 T \leq CK\sigma^2.$$

The way we construct $\sum_{l=1}^T \text{Var}[Y_l]$ is by defining a “merge” operation. Given a continuous summation $\sum_{L=I}^{I+k} X_L$, we will merge the summations using the equation $X_\star = X_{\star_0} + X_{\star_1}$ for any $\star \in \{0,1\}^k$ for $0 \leq k \leq K-1$ as much as possible. For example, summing over all leaves in the left subtree, i.e., $\sum_{L=000\dots 0}^{0111\dots 1} X_L$ can be merged to X_0 . We can merge these summations until no further merging can happen, then we have $\sum_{L=I}^{I+k} X_L = \sum_{l=1}^T Y_l$, where each Y_l is the random variable associated with a (not-necessarily leaf) node in the original tree. It is proven in [Theorem 3.3](#) that each Y_l has variance σ^2 , which confirms Property 1 above. The rest two properties are justified by the two lemmas below. \square

Lemma 3.16. *Let S_1, S_2 be two non-empty subsets of $\{0,1\}^K$ and $S_1 \cap S_2 = \emptyset$. Let $Z_1 := \sum_{i \in S_1} X_i$ and $Z_2 = \sum_{j \in S_2} X_j$, then $\text{Cov}(Z_1, Z_2) \leq 0$. Therefore $\text{Cov}(Y_l, Y_{l'}) \leq 0$ for any $l \neq l'$.*

Proof of [Lemma 3.16](#). We observe $\text{Cov}(Z_1, Z_2) = \sum_{i \in S_1, j \in S_2} \text{Cov}(X_i, X_j)$. Since the covariance matrix $\sigma^2 \mathbf{C}_K$ in [\(3.1\)](#) has only positive entries on the diagonal, but the above summation does not include the diagonal, we conclude $\text{Cov}(Z_1, Z_2) \leq 0$. \square

Lemma 3.17. *Any continuous summation $\sum_{L=I}^{I+k} X_L$ can be merged as a summation $\sum_{l=1}^T Y_l$ with $T \leq 2K-2$ when $K \geq 2$.*

Proof of [Lemma 3.17](#). We first prove any continuous summation of the form $\sum_{L=000\dots 0}^T X_L$ can be merged into at most K summations. The case where $K=1$ is straightforward. Suppose $K=m-1$ is proven, when $K=m$, we pick T such that the summation $\sum_{L=000\dots 0}^T X_L$ has the largest number of summing terms after merging. We may assume without loss of generality that $L \geq 100\dots 0$, as otherwise the summation only happens on the left sub-tree which reduces to our inductive hypothesis. Now we can already split the first left-tree in the summation, and write $\sum_{L=000\dots 0}^T X_L = X_0 + \sum_{L=100\dots 0}^T X_L$. The second term has length at most $m-1$ by inductive hypothesis, as the summation happens at the leftmost node of the right subtree. Therefore the total length is at most m , as claimed. Moreover, the symmetries of the complete binary tree shows any summation of the form $\sum_{L=111\dots 1}^{111\dots 1} X_L$ can also be merged into at most K summations.

Now we prove [Lemma 3.17](#). The $K=2$ case is simple. We assume the claim holds when $K \leq m-1$. When $K=m$, we pick the consecutive summation which has the largest number of terms after merging.

Again, we may assume the summation includes both nodes on the left and right subtree, as otherwise it reduces to the $m - 1$ case. Now we write $\sum_{L=I}^{I+k} X_L = W_1 + W_2$, where W_1 is the summation on the left part ending at the rightmost node of the left subtree, and W_2 on the right part starting at the leftmost node at the right subtree. By our previous induction, both W_1 and W_2 can be merged into a summation of at most $m - 1$ terms. Therefore the whole summation has at most $2m - 2$ terms. \square

These results together give us the upper bound. Now we turn to the lower bound, we will inductively construct a sequence of continuous range summations for each K , and argue the variance scales as $\Theta(K)$.

We first assume K is an odd number, then we consider the consecutive sum by picking the first $M_K := 2^{K-1} + 2^{K-3} + 2^{K-5} + \dots + 1$ entries. Intuitively, we are picking all the left subtree, and the left subtree of the right subtree, and the left subtree of the right subtree of the right subtree, and so on.

Proof of Lemma 3.15, lower bound. For any odd number K , Let

$$V_K := \text{Var} \left[\sum_{k=000\dots 0}^{M_K} X_k \right],$$

where $M_K := 2^{K-1} + 2^{K-3} + 2^{K-5} + \dots + 1$. Then we claim $V_K - V_{K-2} \geq \frac{2}{3}\sigma^2$. Given the claim, we have $V_K/\sigma^2 = \Omega(K)$ for odd K . Since the maximum variance is a non-decreasing function of K , we know

$$\max_{I \in \{0,1\}^K, k \leq 2^K - I} \frac{\text{Var}[\sum_{L=I}^{I+k} X_L]}{\sigma^2} = \Omega(K).$$

To show the claim, we first merge the summation of the these M_K entries, and write

$$\sum_{k=000\dots 0}^{M_K} X_k = \sum_{l=1}^{(K+1)/2} Y_l,$$

where Y_1 is the left subtree, Y_2 is the next summation of 2^{K-3} entries, and so on. Next we define $W_K := \sum_{l=2}^{(K+1)/2} Y_l$. By the recursive structure of our covariance matrix, W_K has variance V_{K-2} . Therefore

$$V_n = \text{Var} \left[\sum_{k=000,\dots,0}^{M_K} X_k \right] = \text{Var}[Y_1 + W_K] = \sigma^2 + V_{K-2} + 2\text{Cov}[Y_1, W_K].$$

The covariance term can be calculated through (3.1), which is $-2^{-2(K-1)-1}\sigma^2|Y_1||W_K|$. Therefore we can further bound V_K as

$$\begin{aligned} V_K &= \text{Var} \left[\sum_{k=000\dots 0}^{M_K} X_k \right] = \text{Var}[Y_1 + W_K] = \sigma^2 + V_{K-2} + 2\text{Cov}[Y_1, W_K] \\ &= \sigma^2 + V_{K-2} - \sigma^2 2^{-2(K-1)} 2^{K-1} M_{K-2} \\ &= \sigma^2 + V_{K-2} - \sigma^2 2^{-(K-1)} (2^{K-3} + 2^{K-5} + \dots + 1) \\ &\geq \sigma^2 + V_{K-2} - \sigma^2 \frac{4}{3} 2^{-(K-1)} 2^{K-3} = V_{K-2} + \frac{2}{3}\sigma^2, \end{aligned}$$

as desired. The last inequality is because

$$\begin{aligned} 2^{K-3} + 2^{K-5} + \dots + 1 &= 2^{K-3} (1 + 1/4 + \dots + 2^{-(K-3)}) \\ &\leq 2^{K-3} (1 + 1/4 + \dots + 2^{-(K-3)} + \dots) \\ &= \frac{4}{3} 2^{K-3}. \end{aligned}$$

\square

With [Lemma 3.15](#) in hand, we are now ready to state the utilities of our privacy mechanism under different metrics.

Theorem 3.18. *Fix $\sigma > 0$ and let query matrix \mathbf{W} be all the continuous range queries, we have:*

- $\text{err}_{\mathbf{W}}^{\infty}(\mathcal{W}_{\sigma}) = \Theta\left(\sigma\sqrt{\log_2(n)}\right)$,
- $\text{err}_{\mathbf{W},2}(\mathcal{W}_{\sigma}) = O\left(\sigma^2 n^2 \log_2(n)\right)$,
- $\text{err}_{\mathbf{W},\infty}(\mathcal{W}_{\sigma}) = O(\sigma \log_2(n))$.

Proof of [Theorem 3.18](#). Recall the classical fact that $\mathbb{E}[|X|] = \sigma\sqrt{2/\pi}$ for $X \sim \mathbb{N}(0, \sigma^2)$, we immediately have:

$$\begin{aligned} \text{err}_{\mathbf{W}}^{\infty}(\mathcal{W}_{\sigma}) &= \left\| \mathbb{E}_{\mathbf{s} \sim \mathbb{N}(\mathbf{0}, \sigma^2 \mathbf{C}_K)}[\|\mathbf{W}\mathbf{s}\|] \right\|_{\infty} \\ &= \sqrt{\frac{2}{\pi}} \max_{I \in \{0,1\}^K, k \leq 2^K - I} \sqrt{\text{Var}\left[\sum_{L=I}^{I+k} X_L\right]} \\ &= \Theta(\sigma\sqrt{K}) \\ &= \Theta\left(\sigma\sqrt{\log_2(n)}\right), \end{aligned}$$

which proves the first claim. The second claim follows immediately from the first claim and [Proposition 3.14](#).

For the last claim, recall the Gaussian tail bound $\mathbb{P}(|X| > t) \leq 2 \exp(-t^2/2\sigma^2)$ given $X \sim \mathbb{N}(0, \sigma^2)$. We can bound the tail probability of the worst-case error as:

$$\begin{aligned} \mathbb{P}_{\mathbf{s} \sim \mathbb{N}(\mathbf{0}, \sigma^2 \mathbf{C}_K)}[\|\mathbf{W}\mathbf{s}\|_{\infty} > t] &= \mathbb{P}\left[\sum_{L=I}^{I+k} X_L > t \text{ for some } I \in \{0,1\}^K, k\right] \\ &\leq \sum_{I,k} \mathbb{P}\left[\sum_{L=I}^{I+k} X_L > t\right] \\ &\leq 2 \sum_{I,k} \exp\left(\frac{-t^2}{2\text{Var}(\sum_{L=I}^{I+k} X_L)}\right) \\ &\leq 2 \sum_{I,k} \exp\left(\frac{-t^2}{2 \max \text{Var}(\sum_{L=I}^{I+k} X_L)}\right) \\ &\leq 2 \binom{n}{2} \exp\left(\frac{-t^2}{2c\sigma^2 K}\right) \\ &\leq n^2 \exp\left(\frac{-t^2}{2c\sigma^2 K}\right). \end{aligned}$$

Here the first inequality follows from the union bound, and the summation is over all the continuous range queries (and therefore $\binom{n}{2}$ terms). The second inequality uses the Gaussian tail bound. The last few inequalities use [Lemma 3.15](#).

Now set $t_m = m\sqrt{4 \log(n) c \sigma^2 K}$ for every positive integer m , we know

$$\begin{aligned} \mathbb{P}_{\mathbf{s} \sim \mathbb{N}(\mathbf{0}, \sigma^2 \mathbf{C}_K)}[\|\mathbf{W}\mathbf{s}\|_{\infty} > t_m] &\leq n^2 \exp\left(\frac{-t_m^2}{2c\sigma^2 K}\right) \\ &= n^2 \exp\left(\frac{-4m^2 \log(n) c \sigma^2 K}{2c\sigma^2 K}\right) \\ &= n^2 \exp(-2m^2 \log(n)) \\ &= \frac{1}{n^{2m^2 - 2}}. \end{aligned}$$

Therefore we can bound

$$\begin{aligned}
\text{err}_{\mathbf{W},\infty}(\mathcal{W}_\sigma) &= \mathbb{E}_{\mathbf{s} \sim \mathbb{N}(\mathbf{0}, \sigma^2 \mathbf{C}_K)} [\|\mathbf{W}\mathbf{s}\|_\infty] \\
&= \int_0^\infty \mathbb{P}_{\mathbf{s} \sim \mathbb{N}(\mathbf{0}, \sigma^2 \mathbf{C}_K)} [\|\mathbf{W}\mathbf{s}\|_\infty > t] dt \\
&\leq t_1 + \sum_{m=1}^\infty \int_{t_m}^{t_{m+1}} \mathbb{P}_{\mathbf{s} \sim \mathbb{N}(\mathbf{0}, \sigma^2 \mathbf{C}_K)} [\|\mathbf{W}\mathbf{s}\|_\infty > t] dt \\
&\leq \sqrt{4 \log(n) c \sigma^2 K} + \sqrt{4 \log(n) c \sigma^2 K} \sum_{m=1}^\infty \mathbb{P}_{\mathbf{s} \sim \mathbb{N}(\mathbf{0}, \sigma^2 \mathbf{C}_K)} [\|\mathbf{W}\mathbf{s}\|_\infty > t_m] \\
&= \sqrt{4 \log(n) c \sigma^2 K} + \sqrt{4 \log(n) c \sigma^2 K} \sum_{m=1}^\infty \frac{1}{n^{2m^2-2}} \\
&= O(\sqrt{4 \log(n) c \sigma^2 K}) = O(\sigma \log(n)) \quad \text{as } K = \log_2(n).
\end{aligned}$$

□

When selecting σ to comply with the privacy budget, the next corollary gives the utility guarantee for our mechanism, which is immediate by plugging the value of σ from [Theorem 3.8](#) into [Theorem 3.18](#).

Corollary 3.19. *Let $X \in \mathcal{X}^n$ be any dataset and let $\mathcal{M}_\sigma(X) = X + \sigma \mathbb{N}(\mathbf{0}, \mathbf{C}_K)$ be our privacy mechanism, where σ is chosen such that the mechanism satisfies (ε, δ) -DP. Let \mathbf{W} be all the continuous range queries, we have:*

- $\text{err}_{\mathbf{W}}^\infty(\mathcal{W}_\sigma) = \Theta\left(\log(n) \sqrt{\log(2/\delta)} \varepsilon^{-1}\right)$,
- $\text{err}_{\mathbf{W},2}(\mathcal{W}_\sigma) = O\left(n^2 \log^2(n) \log(2/\delta) \varepsilon^{-2}\right)$,
- $\text{err}_{\mathbf{W},\infty}(\mathcal{W}_\sigma) = O\left(\log^{1.5}(n) \sqrt{\log(2/\delta)} \varepsilon^{-1}\right)$.

[Theorem 3.18](#) differs from the scenario where independent Gaussian noise $\mathbb{N}(0, \sigma^2)$ is added to each leaf node. In the latter case, the three errors, $\text{err}_{\mathbf{W},2}$, $\text{err}_{\mathbf{W}}^\infty$, and $\text{err}_{\mathbf{W},\infty}$, are $\Theta(n^3 \sigma^2)$, $\Theta(\sqrt{n} \sigma)$, and $\Omega(\sqrt{n} \sigma)$ respectively. In contrast, our mechanism results in errors of $\Theta(n^2 \log(n) \sigma^2)$, $O(\sqrt{\log(n)} \sigma)$, and $O(\log(n) \sigma)$, indicating lower error magnitudes for all evaluated metrics.

Comparison of bounds in [Corollary 3.19](#): The bounds attained by our mechanism for $\text{err}_{\mathbf{W},2}(\mathcal{W}_\sigma)$ match previous work [Hay et al. \(2010\)](#); [Xiao et al. \(2011\)](#) which can be viewed as instantiation of matrix mechanism [Li et al. \(2015\)](#). To our knowledge, this is the first work that obtains comparable bound to specialized output perturbation mechanisms for range queries. We also show that empirically we match the performance of these methods in [Section 4](#). Though these works do not explicitly analyze for $\text{err}_{\mathbf{W},\infty}(\mathcal{W}_\sigma)$, [Jain et al. \(2023\)](#) showed that the Binary Tree mechanism [Dwork et al. \(2010\)](#); [Chan et al. \(2011\)](#) with Gaussian noise obtains the same $O(\log^{3/2} n)$ bound.

In terms of tightness, our bound for $\text{err}_{\mathbf{W},2}(\mathcal{W}_\sigma)$ is optimal among all (ε, δ) -DP mechanisms. To see this, note that the workload matrix for continual counting (a lower triangular matrix of size $n \times n$ with 1 for entries on and below the diagonal and 0 elsewhere) forms a subset of the workload matrix for continuous queries. [Henzinger et al. \(2023\)](#) (Thm. 4) show $\Omega(\log^2 n)$ lower bound on error for any (ε, δ) -DP mechanism for the continual counting which matches our upper bound (after scaling for number of queries). For $\text{err}_{\mathbf{W},\infty}(\mathcal{W}_\sigma)$, [Fichtenberger et al. \(2023\)](#) (Thm. 3) show $\Omega(\log^2 n)$ lower bound on the *squared-infinity* error for any (ε, δ) -DP mechanism, leading to an $\Omega(\log n)$ lower bound for $\text{err}_{\mathbf{W},\infty}(\mathcal{W}_\sigma)$. Consequently, our upper bound for $\text{err}_{\mathbf{W},\infty}(\mathcal{W}_\sigma)$ in [Corollary 3.19](#) is only off by a factor of $\log^{0.5} n$ (due to Gaussian concentration) compared to the known lower bound. An intriguing open question is whether this gap can be narrowed from either side.

3.4.2 Node queries

When \mathbf{W} represents the queries for all the nodes in the binary tree. Our results are summarized below:

Theorem 3.20. Fix $\sigma > 0$ and let query matrix \mathbf{W} be all the nodal queries, we have:

- $\text{err}_{\mathbf{W}}^{\infty}(\mathcal{W}_{\sigma}) = \sqrt{2/\pi}\sigma,$
- $\text{err}_{\mathbf{W},2}(\mathcal{W}_{\sigma}) = (2n - 1)\sigma^2,$
- $\text{err}_{\mathbf{W},\infty}(\mathcal{W}_{\sigma}) = O(\sigma\sqrt{\log_2(n)}).$

Proof of Theorem 3.20. The first two properties are follows from direct calculation, and are therefore omitted here.

The proof for the worst-case expected error is very similar to the calculation in Theorem [Theorem 3.18](#). Recall that all the leaf nodes are labelled by X_I where $I \in \{0, 1\}^K$ which has covariance matrix $\sigma^2\mathbf{C}_K$. The internal nodes are labelled by X_J where $J \in \{0, 1\}^k$ for some $k \in \{0, 1, \dots, K - 1\}$. Therefore $\text{err}_{\mathbf{W},\infty}(\mathcal{W}_{\sigma}) = \mathbb{E}[\max_{k,J}|X_J|, J \in \{0, 1\}^k]$. We can again use the standard Gaussian concentration:

$$\begin{aligned} \mathbb{P}[\max_{k,J}|X_J| > t] &= \mathbb{P}[|X_J| > t \text{ for some } J \in \{0, 1\}^k] \\ &\leq \sum_{J,k} \mathbb{P}[|X_J| > t] \\ &= (2n - 1) \exp\left(\frac{-t^2}{2\sigma^2}\right) \quad \text{total } 2n - 1 \text{ summation terms.} \end{aligned}$$

Now set $t_m = m\sqrt{2\sigma^2 \log(n)}$, we know

$$\mathbb{P}[\max_{k,J}|X_J| > t_m] \leq \frac{(2n - 1)}{n^{m^2}}.$$

Therefore

$$\begin{aligned} \text{err}_{\mathbf{W},\infty}(\mathcal{W}_{\sigma}) &= \int_0^{\infty} \mathbb{P}[\max_{k,J}|X_J| > t] dt \\ &= \sqrt{2\sigma^2 \log(n)} + \sqrt{2\sigma^2 \log(n)} \sum_{m=1}^{\infty} \frac{(2n - 1)}{n^{m^2}} \\ &= O(\sigma\sqrt{\log(n)}), \end{aligned}$$

as announced. □

We obtain the following corollary substituting the value of σ from [Theorem 3.8](#).

Corollary 3.21. Let $X \in \mathcal{X}^n$ be any dataset and let $\mathcal{M}_{\sigma}(X) = X + \sigma\mathbb{N}(\mathbf{0}, \mathbf{C}_K)$ be our privacy mechanism, where σ is chosen such that the mechanism satisfies (ϵ, δ) -DP. Let \mathbf{W} be all the continuous range queries, we have:

- $\text{err}_{\mathbf{W}}^{\infty}(\mathcal{W}_{\sigma}) = \Theta\left(\sqrt{\log n \log(2/\delta)}\epsilon^{-1}\right),$
- $\text{err}_{\mathbf{W},2}(\mathcal{W}_{\sigma}) = \Theta\left(n^2 \log(n) \log(2/\delta)\epsilon^{-2}\right),$
- $\text{err}_{\mathbf{W},\infty}(\mathcal{W}_{\sigma}) = O\left(\log(n)\sqrt{\log(2/\delta)}\epsilon^{-1}\right).$

4 Experiments

In this section we demonstrate numerical experiments to showcase efficiency of the sampling algorithm and improved utility obtained by our correlated mechanism.

4.1 Efficiency of cascade sampling

To justify the practical efficiency of our cascade sampling in [Section 3.2](#), we compare our algorithm against `Scipy`'s built-in function for generating multivariate Gaussian distributions. On a personal laptop, we use both methods to produce Gaussians with a covariance matrix C_k for $k \in \{3, 4, \dots, 25\}$, which corresponds to dimensionalities ranging from $2^3 = 8$ to $2^{25} \approx 33.5$ million. The computational costs in terms of clock time for both scales—original and logarithmic—are displayed in [Fig. 3](#). Our Cascade Sampling algorithm demonstrates remarkable efficiency, requiring less than a second for dimensionalities up to 2^{17} (131,072). Even for a over 33.5 million-dimensional Gaussian, our algorithm completes the task in under 9 minutes. The right part of [Fig. 3](#) features a scatter plot of $\log(\text{Time})$ against $\log(\text{Data Points})$, with a fitted straight line that has a slope of 1.05, closely aligning with 1, confirming our theoretical assertion of linear cost. In comparison, `Scipy`'s `multivariate_normal` function consistently takes longer time. Its efficiency diminishes at higher dimensions. For example, it takes over 28 minutes to sample a 16,384 (2^{14})-dimensional Gaussian, and more than 3 hours for a 32,768 (2^{15})-dimensional Gaussian, making it impractical for larger dimensions. Samplers from other libraries like `Numpy` were also tested but could not execute for dimensions exceeding 1024.

4.2 Utility comparison with existing algorithms

We evaluate the correlated input perturbation mechanism against the Gaussian (adding noise to \mathbf{x} and querying from the privatized data), Binary Tree [Dwork et al. \(2010\)](#); [Chan et al. \(2011\)](#), Hierarchical [Hay et al. \(2010\)](#), Wavelet [Xiao et al. \(2011\)](#) and EigenDesign mechanisms [Li and Miklau \(2012\)](#). We do not compare with a Gaussian mechanism that privatizes the output queries (adding noise to $\mathbf{W}\mathbf{x}$) as this performs

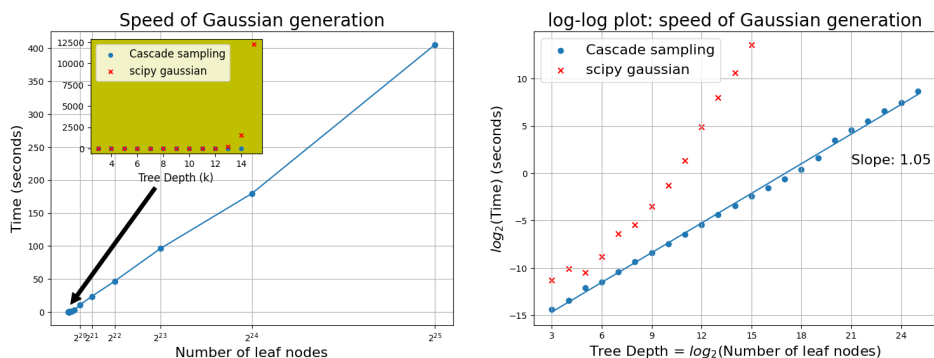


Figure 3: Comparison of Gaussian Generation Speeds. The left plot is in the original scale, the right is in the log-log scale.

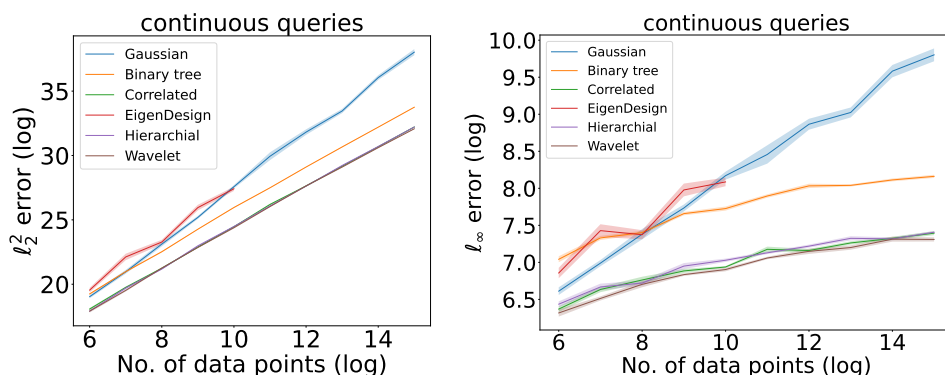


Figure 4: $\text{err}_{\mathbf{W},2}(\mathcal{W}_\sigma)$ and $\text{err}_{\mathbf{W},\infty}(\mathcal{W}_\sigma)$ for continuous queries.

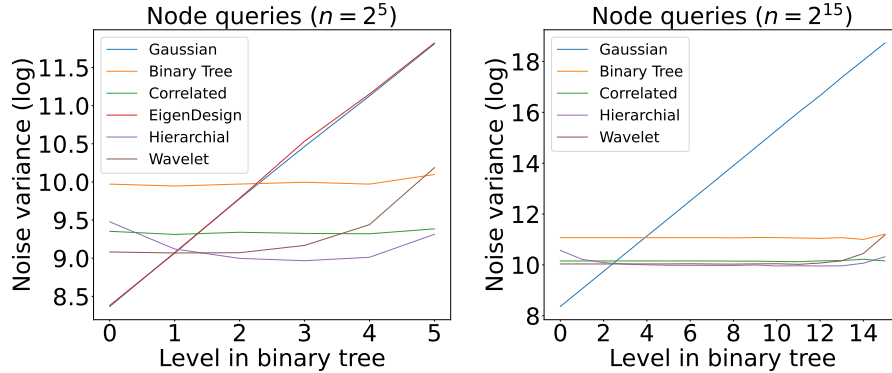


Figure 5: Variance (log) of queries for levels of binary tree.

substantially worse due to high sensitivity. Experiments comparing runtime are in [Appendix C.3](#).

Experimental setup: We compare mechanisms on randomly generated data, where each element of $\mathbf{x} \in \mathbb{Z}^n$ is sampled uniformly at random from 1 to 1000. We consider the case where a person contributes a single count to an element in \mathbf{x} and hence for neighboring \mathbf{x} and \mathbf{x}' , $\|\mathbf{x} - \mathbf{x}'\|_1 = 1$. We consider n in range $\{2^6, \dots, 2^{15}\}$, except for EigenDesign which we restrict to 2^{10} due to computational overhead. We fix privacy parameters $\epsilon = 0.1$ and $\delta = 10^{-9}$ for all our experiments and report $\text{err}_{\mathbf{W},2}(\mathcal{W}_\sigma)$ and $\text{err}_{\mathbf{W},\infty}(\mathcal{W}_\sigma)$ ([Definition 3.11](#) and [Definition 3.13](#)) for different choices of workload matrices \mathbf{W} . The error values on graphs are plotted with ± 0.25 standard deviation across 10 independent runs for all experiments. Experiments for node and random queries and additional implementation details are included in [Appendix C](#).

Continuous range queries: A continuous range query is specified by start and end index in $\{1, \dots, n\}$ and the answer is sum of all elements within this range. We consider the workload matrix of all possible $\binom{n}{2} + n$ queries. As for large n computing output of all these queries becomes computationally infeasible, we instead randomly sample the queries to obtain a Monte Carlo estimate of the errors, with details explained in [Appendix C.4](#). We sample 5000 queries for each value of n in $\{2^6, \dots, 2^{15}\}$ and report estimated $\text{err}_{\mathbf{W},2}(\mathcal{W}_\sigma)$ and $\text{err}_{\mathbf{W},\infty}(\mathcal{W}_\sigma)$ in [Fig. 4](#).

The error follows roughly the same trend for $\text{err}_{\mathbf{W},2}(\mathcal{W}_\sigma)$ and $\text{err}_{\mathbf{W},\infty}(\mathcal{W}_\sigma)$. Wavelet has the smallest error, closely followed by our mechanism and Hierarchical. For small n , Gaussian mechanism performs as well as these methods but suffers variance scaling linearly in n for larger values. Our mechanism, owing to its design, exhibits significantly reduced error compared to the standard Gaussian approach, its primary local DP competitor. Our method’s error is only marginally higher than Wavelet. Nevertheless, it maintains advantageous statistical properties such as unbiasedness, consistency, and transparency.

Utility control: The ability to control noise variance across different ‘levels’ of summation was one of the motivations of our mechanism, which we demonstrate here. We consider a binary tree over the dataset vector \mathbf{x} , and the queries (which are nodes of the tree) correspond to intervals summing up the leaves of the sub-tree rooted at the node. We then consider the variance of noise across queries corresponding to different levels (and the root would correspond to the highest level summing up all the elements of \mathbf{x}). We perform this for $n = 2^5$ and $n = 2^{15}$ for 500 independent runs and the results are shown in [Fig. 5](#).

As the additive correlated noise in our mechanism is designed to have the same variance across levels, our mechanism and the Binary Tree mechanism, which adds i.i.d. Gaussian noises to each element of binary tree to answer queries have the same variance across all such queries. Comparatively, Gaussian and EigenDesign have variance linearly increasing across levels. Wavelet has smaller consistent variance for smaller levels (corresponding to short ranges) but increases sharply for long ranges. Hierarchical has the smallest variance in magnitude and also a typical trend — variance is larger for smaller and larger levels and less for intermediate ones, which helps illustrate the effect of post-processing and explain the improved utility.

5 Discussion and Future Work

Our proposal permits straightforward generalizations to general binary trees (that is, all branches of the tree need not have the same depth), as well as higher-dimensional query types, in particular 2-D range queries and contingency tables that recognize, for example, the geographic contiguity of the data points. Both generalizations call for modifications to the noise allocation scheme in the cascade sampling algorithm. Appendices B.1 and B.2 respectively discuss the approaches to instantiate these generalizations.

The proposed local DP mechanism leverages error correlation structures which, once combined with the query workload matrix, allows for fine-grained control over error magnitude across queries at different geographic levels, a feature that is highly desirable in applications such as the dissemination of structured and complex official statistics. We believe this work leads to a generic framework of differential privacy mechanism design. When the data or query workload structure is well understood, additional benefits can result from catering privacy perturbations to respect these known structures. This investigation is left to future work.

References

- Abowd, J. M., Ashmead, R., Cumings-Menon, R., Garfinkel, S., Heineck, M., Heiss, C., Johns, R., Kifer, D., Leclerc, P., Machanavajjhala, A., Moran, B., Sexton, W., Spence, M., and Zhuravlev, P. (2022). The census topdown algorithm. *Harvard Data Science Review*.
- Barak, B., Chaudhuri, K., Dwork, C., Kale, S., McSherry, F., and Talwar, K. (2007). Privacy, accuracy, and consistency too: a holistic solution to contingency table release. In *Proceedings of the twenty-sixth ACM SIGMOD-SIGACT-SIGART symposium on Principles of database systems*, pages 273–282.
- Canonne, C. L., Kamath, G., and Steinke, T. (2020). The discrete gaussian for differential privacy. *Advances in Neural Information Processing Systems*, 33:15676–15688.
- Chan, T.-H. H., Shi, E., and Song, D. (2011). Private and continual release of statistics. *ACM Trans. Inf. Syst. Secur.*, 14(3).
- Dharangutte, P., Gao, J., Gong, R., and Yu, F.-Y. (2023). Integer subspace differential privacy. *Proceedings of the The Thirty-Seventh AAAI Conference on Artificial Intelligence (AAAI-23)*. arXiv:2212.00936.
- Dinur, I. and Nissim, K. (2003). Revealing information while preserving privacy. In *Proceedings of the Twenty-Second ACM SIGMOD-SIGACT-SIGART Symposium on Principles of Database Systems*, PODS '03, page 202–210, New York, NY, USA. Association for Computing Machinery.
- Dwork, C., McSherry, F., Nissim, K., and Smith, A. (2006). Calibrating noise to sensitivity in private data analysis. In *Proceedings of the Third Conference on Theory of Cryptography, TCC'06*, page 265–284, Berlin, Heidelberg. Springer-Verlag.
- Dwork, C., Naor, M., Pitassi, T., and Rothblum, G. N. (2010). Differential privacy under continual observation. In Schulman, L. J., editor, *Proceedings of the 42nd ACM Symposium on Theory of Computing, STOC 2010, Cambridge, Massachusetts, USA, 5-8 June 2010*, pages 715–724. ACM.
- Dwork, C. and Nissim, K. (2004). Privacy-Preserving datamining on vertically partitioned databases. In *Advances in Cryptology – CRYPTO 2004*, pages 528–544. Springer Berlin Heidelberg.
- Dwork, C. and Roth, A. (2014). The algorithmic foundations of differential privacy. *Foundations and Trends® in Theoretical Computer Science*, 9(3–4):211–407.
- Fichtenberger, H., Henzinger, M., and Upadhyay, J. (2023). Constant matters: Fine-grained error bound on differentially private continual observation. In Krause, A., Brunskill, E., Cho, K., Engelhardt, B., Sabato, S., and Scarlett, J., editors, *International Conference on Machine Learning, ICML 2023, 23-29 July 2023, Honolulu, Hawaii, USA*, volume 202 of *Proceedings of Machine Learning Research*, pages 10072–10092. PMLR.

- Fioretto, F. and Van Hentenryck, P. (2019). Differential privacy of hierarchical census data: An optimization approach. In *International Conference on Principles and Practice of Constraint Programming*, pages 639–655. Springer.
- Gao, J., Gong, R., and Yu, F.-Y. (2022). Subspace differential privacy. In *Proceedings of the The Thirty-Sixth AAAI Conference on Artificial Intelligence (AAAI-22)*, pages 3986–3995. arXiv:2108.11527.
- Gong, R. (2022). Transparent privacy is principled privacy. *Harvard Data Science Review (Special Issue 2)*. doi:10.1162/99608f92.b5d3faaa.
- Hardt, M., Ligett, K., and McSherry, F. (2012). A simple and practical algorithm for differentially private data release. *Adv. Neural Inf. Process. Syst.*, 25.
- Hardt, M. and Talwar, K. (2010). On the geometry of differential privacy. In *Proceedings of the forty-second ACM symposium on Theory of computing*, pages 705–714.
- Hay, M., Machanavajjhala, A., Miklau, G., Chen, Y., Zhang, D., and Bissias, G. (2016). Exploring privacy-accuracy tradeoffs using dpcomp. In Özcan, F., Koutrika, G., and Madden, S., editors, *Proceedings of the 2016 International Conference on Management of Data, SIGMOD Conference 2016, San Francisco, CA, USA, June 26 - July 01, 2016*, pages 2101–2104. ACM.
- Hay, M., Rastogi, V., Miklau, G., and Suci, D. (2010). Boosting the accuracy of differentially private histograms through consistency. *Proceedings VLDB Endowment*, 3(1-2):1021–1032.
- Henzinger, M., Upadhyay, J., and Upadhyay, S. (2023). Almost tight error bounds on differentially private continual counting. In Bansal, N. and Nagarajan, V., editors, *Proceedings of the 2023 ACM-SIAM Symposium on Discrete Algorithms, SODA 2023, Florence, Italy, January 22-25, 2023*, pages 5003–5039. SIAM.
- Honaker, J. (2015). Efficient use of differentially private binary trees. *Theory and Practice of Differential Privacy (TPDP 2015), London, UK*, 2:26–27.
- Jain, P., Raskhodnikova, S., Sivakumar, S., and Smith, A. D. (2023). The price of differential privacy under continual observation. In Krause, A., Brunskill, E., Cho, K., Engelhardt, B., Sabato, S., and Scarlett, J., editors, *International Conference on Machine Learning, ICML 2023, 23-29 July 2023, Honolulu, Hawaii, USA*, volume 202 of *Proceedings of Machine Learning Research*, pages 14654–14678. PMLR.
- Li, C. and Miklau, G. (2012). An adaptive mechanism for accurate query answering under differential privacy. *Proc. VLDB Endow.*, 5(6):514–525.
- Li, C., Miklau, G., Hay, M., McGregor, A., and Rastogi, V. (2015). The matrix mechanism: optimizing linear counting queries under differential privacy. *The VLDB journal*, 24(6):757–781.
- McKenna, L. (2018). Disclosure avoidance techniques used for the 1970 through 2010 decennial censuses of population and housing. Technical report, U. S. Census Bureau.
- Muthukrishnan, S. and Nikolov, A. (2012). Optimal private halfspace counting via discrepancy. In *Proceedings of the forty-fourth annual ACM symposium on Theory of computing*, pages 1285–1292.
- Nikolov, A., Talwar, K., and Zhang, L. (2013). The geometry of differential privacy: the sparse and approximate cases. In *Proceedings of the forty-fifth annual ACM symposium on Theory of computing*, pages 351–360. ACM.
- Qardaji, W. H., Yang, W., and Li, N. (2013). Understanding hierarchical methods for differentially private histograms. *Proc. VLDB Endow.*, 6(14):1954–1965.
- Seeman, J., Slavkovic, A., and Reimherr, M. (2022). A formal privacy framework for partially private data. *arXiv preprint arXiv:2204.01102*.

U.S. Census Bureau (2022). Technical documentation – operational quality metrics, last updated 10.06.22. Technical report, U.S. Census Bureau.

Xiao, X., Wang, G., and Gehrke, J. (2011). Differential privacy via wavelet transforms. *IEEE Trans. Knowl. Data Eng.*, 23(8):1200–1214.

A An extended review of related literature

Linear query is a central topic that has been studied extensively in the differential privacy literature. To supplement the brief review provided in [Section 2.3](#), we discuss in greater detail existing work on privacy mechanisms for linear queries in relation to the properties of unbiasedness, consistency, statistical transparency, and flexible utility control.

A simplest mechanism is a locally differentially private mechanism in which each data entry is either perturbed (in a discrete setting) or infused with an independent noise (often from a Laplace or Gaussian distribution) with suitable magnitude. The linear query can be answered by simply reporting the query answer on the perturbed data. As [Section 2.3](#) alludes to, local DP supports unbiasedness, logical consistency, statistical transparency, and are exceptionally amenable to distributed implementation. However, local privacy does not support flexible utility specifications. In particular, when a query range contains a large number of data elements, the query utility (or error) grows in the order of $O(\sqrt{n})$ where n is the the number of elements in the range. The error blow-up for aggregated data substantially hinders the use of local DP in practice, even though it is known to give excellent privacy protection.

In contrast to local DP, which is often termed *input* perturbation since noise is directly added to the input data elements, mechanisms that use *output* perturbation consider adding noise to the query output. One classic example is the Gaussian mechanism [Dinur and Nissim \(2003\)](#); [Dwork and Nissim \(2004\)](#); [Dwork et al. \(2006\)](#). The variance of independent Gaussian noise added to each query needs to be tailored to the query *sensitivity*, i.e., the maximum number of queries one element is involved, or the largest norm of the columns of workload matrix \mathbf{W} . Gaussian mechanisms satisfy unbiasedness and statistical transparency, but does not support consistency nor utility control.

The noise magnitude could be high when the sensitivity of \mathbf{W} is high.

A notable class of Gaussian mechanisms provide improved utility to linear queries by leveraging their geometric structure [Hardt and Talwar \(2010\)](#); [Nikolov et al. \(2013\)](#).

Specifically, consider the workload matrix W as a linear map that maps the input data histogram to a d -dimensional output vector, with $d \ll n$. [Hardt and Talwar \(2010\)](#) studied the image of the unit ℓ_1 ball under the linear map \mathbf{W} (which is a convex polytope K) and use an instantiation of the exponential mechanism (via a randomly chosen point in K) for ϵ -differential privacy. In a later work, [Nikolov et al. \(2013\)](#) considered the setting when the number of queries d is much larger than n , and (ϵ, δ) -differential privacy in general. They use a Gaussian mechanism where the parameters are guided by the minimum enclosing ellipsoid of a square submatrix of \mathbf{W} . These mechanisms have polylogarithmic approximation (in terms of error) to the lower bound for such queries, which are derived by using hereditary discrepancy of \mathbf{W} . As special cases of Gaussian mechanisms, these mechanisms also fall in the category of output perturbation, and enjoy similar properties as does the classic Gaussian mechanism in terms of bias, consistency, transparency, and utility control.

The matrix mechanism by [Li et al. \(2015\)](#) is a workload-dependent mechanism in that it is constructed by using the workload matrix \mathbf{W} . As [Section 2.3](#) discusses, the mechanism is situated somewhere in between input and output perturbation. Specifically, the workload matrix \mathbf{W} is factored into two matrices R and A , with R called the reconstruction matrix and A the strategy matrix. Gaussian errors are added to the intermediate result Ah , where h is the histogram vector. The final query result is taken as the multiplication of R and the noisy intermediate result. This way the sensitivity can be controlled by the maximum column norm of A and final query error is proportional to the max row norm of R and maximum column norm of A . By choosing an appropriate factorization $\mathbf{W} = RA$ (e.g., by using convex optimization), one can get near optimal utility that is within $O(\log^2 n)$ to the optimal error of any data-independent mechanism [Nikolov et al. \(2013\)](#). The matrix mechanism is unbiased, has statistical transparency and again fails at consistency and utility control.

A number of prior work considered range query problems and developed hierarchical methods, which can be considered as special cases of the matrix mechanism [Hay et al. \(2010\)](#); [Chan et al. \(2011\)](#); [Qardaji et al. \(2013\)](#); [Xiao et al. \(2011\)](#); [Honaker \(2015\)](#). We use [Chan et al. \(2011\)](#) as an example to illustrate the main idea. [Chan et al. \(2011\)](#) considered a specific type of range query that is derived from continuous counting in a data stream. Specifically, consider a set of binary data points $x_i \in \{0, 1\}$ arriving sequentially, the goal is to report the count at any time t , i.e., $X_t = \sum_{i=1}^t x_i$, for all t , with differential privacy guarantee for individual data points. They developed a mechanism that renders the error utility of bound $O((1/\epsilon) \log^{3/2} t)$ for answering the t -th counting query with ϵ -differential privacy. The main idea is to maintain a binary tree on the data stream x_1, \dots, x_t and add an independent Laplace noise for each internal node in the binary tree. The final query output will be derived by the summation of the (noisy) count of selected vertices in the binary tree. The mechanism can be applied to a general 1D range query problem of reporting $\sum_{k=i}^j x_k$, for any 1D range $[i, j]$, with $i \leq j$, with the same error bound. It meets unbiasedness and statistical transparency but does not have consistency and utility flexibility. A number of other work use similar ideas: [Barak et al. \(2007\)](#) uses subsets of Fourier basis, [Xiao et al. \(2011\)](#) uses wavelet transforms, and [Muthukrishnan and Nikolov \(2012\)](#) considers general range queries with constant VC-dimension (e.g., half-space queries).

Though not part of the comparison presented in [Table 1](#), we make a brief comment on the practicality of implementation. Among the mechanisms discussed here and in [Section 2.3](#), some are mainly of theoretical interest [Hardt et al. \(2012\)](#); [Nikolov et al. \(2013\)](#); [Muthukrishnan and Nikolov \(2012\)](#). The matrix mechanism has a practical instantiation [McKenna \(2018\)](#), as does [Hay et al. \(2010\)](#) and the subspace DP mechanisms of [Gao et al. \(2022\)](#); [Dharangutte et al. \(2023\)](#). In addition, the TopDown algorithm has been extensively instantiated, though it is difficult to independently replicate due to its formidable scale.

B Generalizations

B.1 General binary trees

Our noise mechanism is designed under the assumption that our data points can be viewed as leaves of a perfect binary tree. Nevertheless, thank to the top-down nature of our cascade sampling algorithm ([Algorithm 1](#)), it can be readily adapted to work with a general binary tree. We will still use binary bits to represent data points. They are still leaves of a binary tree of maximum depth k , but not necessarily have the same depth (i.e., same length in the bit string). In our binary tree, the root node is still indexed by \emptyset . For any non-leaf node identified by the bit string \star , its children are indexed as $\star 0$ and $\star 1$ if it has two children, or solely as $\star 0$ if it has only one child.

Our adapted algorithm closely mirrors [Algorithm 1](#), with the primary distinction being the evaluation of the number of children at each step. Starting from the root, the process proceeds downward. Given the assigned value to a node \star , the algorithm first determines the number of \star 's children. If \star has two children, it generates correlated noises in the same way as [Algorithm 1](#) (or as described in formula 2). If \star has only one child, the same noise is assigned to $\star 0$. If \star is itself a leaf, the algorithm simply moves on to the next node. Detailed description is in [Algorithm 2](#) below.

[Algorithm 2](#) continues to ensure that the marginal distributions for each node adhere to $\mathbb{N}(0, \sigma^2)$. Moreover, the noise level for any given node is equivalent to the sum of the noise levels of its children, thereby maintaining consistency. The theoretical analysis for this scenario closely parallels that of the perfect binary tree case discussed in [Section 3](#). Extending this approach to non-binary trees is also possible, though more complicated. This further exploration will be reserved for our future studies.

B.2 Two-dimensional range queries and contingency tables

Remember that our approach, as outlined in [Algorithm 1](#), is appropriate for data arranged in one-dimensional arrays that have hierarchical structures. We are now expanding this method to apply to two-dimensional contingency tables. An example of this is that each data point represents the population of a village, positioned in two dimensions for longitude and latitude. The higher-level hierarchies might represent the populations of larger entities like cities, provinces, or countries.

Putting it formally, we consider data points labeled as $\{X_{I,J}\}_{I \in \{0,1\}^{k_1}, J \in \{0,1\}^{k_2}}$. It is convenient to think

Algorithm 2 Noise Allocation Mechanism for a General Binary Tree

Input: Binary tree with maximum depth k , variance σ^2 determined by the privacy budget.

Output: Noise values $\{X_I\}$ for all nodes $I \in \cup_{0 \leq l \leq k} \{0, 1\}^l$ in a binary tree.

for each node $\star \in \{0, 1\}^i$ at depth $0 \leq i \leq k - 1$ **do**

if $\star = \emptyset$ **then**

 Assign $X_{\emptyset} \sim \mathbb{N}(0, \sigma^2)$

 Sample $Y_{\star} \sim \mathbb{N}(0, \sigma^2)$ independently

 Define the noise values for the children nodes of \star :

if \star has two children **then**

$$X_{\star 0} := \frac{1}{2}X_{\star} + \frac{\sqrt{3}}{2}Y_{\star}$$

end if

$$X_{\star 1} := \frac{1}{2}X_{\star} - \frac{\sqrt{3}}{2}Y_{\star}$$

else if \star has one child **then**

$$X_{\star 0} = X_{\star}$$

end if

end for

of these data points as elements of a matrix with 2^{k_1} rows and 2^{k_2} columns. Each row and column corresponds to the leaf nodes of a perfect binary tree of heights k_1 and k_2 , respectively. Each pair of (internal) nodes (I_1, J_1) from the two binary trees represents a submatrix. For instance, the pair (\emptyset, \emptyset) corresponds to the entire data matrix. We aim to develop a noise mechanism where the summation of noises applied to each submatrix, as described by $(I_1, J_1)_{I_1 \in \{0,1\}^{i_1}, J_2 \in \{0,1\}^{i_2}, i_1 \leq k_1, i_2 \leq k_2}$, maintain the same variance.

Remember that for the one-dimensional scenario, the essence of our design hinges on the observation that if $X, Y \sim \mathbb{N}(0, 1)$, then the variables X_0, X_1 given by

$$X_0 = \frac{1}{2}X + \frac{\sqrt{3}}{2}Y, \quad X_1 = \frac{1}{2}X - \frac{\sqrt{3}}{2}Y.$$

also follow a $\mathbb{N}(0, 1)$ distribution. The above construction can be generalized to higher dimensions. For example, let X, Y, Z, W be i.i.d. $\mathbb{N}(0, 1)$ random variables, and define:

$$\begin{aligned} X_0 &= \frac{1}{2}X + \frac{\sqrt{3}}{2}Y, & X_1 &= \frac{1}{2}X - \frac{\sqrt{3}}{2}Y \\ \tilde{X}_0 &= \frac{1}{2}Z + \frac{\sqrt{3}}{2}W, & \tilde{X}_1 &= \frac{1}{2}Z - \frac{\sqrt{3}}{2}W. \end{aligned}$$

Then we can construct

$$\begin{aligned} (X_{00}, X_{01}) &= \frac{1}{2}(X_0, X_1) + \frac{\sqrt{3}}{2}(\tilde{X}_0, \tilde{X}_1) \\ (X_{10}, X_{11}) &= \frac{1}{2}(X_0, X_1) - \frac{\sqrt{3}}{2}(\tilde{X}_0, \tilde{X}_1), \end{aligned}$$

or equivalently

$$\begin{aligned} X_{00} &= \frac{1}{4}X + \frac{\sqrt{3}}{4}Y + \frac{\sqrt{3}}{4}Z + \frac{3}{4}W \\ X_{01} &= \frac{1}{4}X - \frac{\sqrt{3}}{4}Y + \frac{\sqrt{3}}{4}Z - \frac{3}{4}W \\ X_{10} &= \frac{1}{4}X + \frac{\sqrt{3}}{4}Y - \frac{\sqrt{3}}{4}Z - \frac{3}{4}W \\ X_{11} &= \frac{1}{4}X - \frac{\sqrt{3}}{4}Y - \frac{\sqrt{3}}{4}Z + \frac{3}{4}W. \end{aligned}$$

We can verify that the matrix

$$\begin{pmatrix} X_{00} & X_{01} \\ X_{10} & X_{11} \end{pmatrix}$$

satisfies the following:

- Each entry is a standard normal
- The summations of each row, each column are all standard normals
- The summation of all entries are standard normals.
- $X_{00} + X_{10} = X_0, X_{01} + X_{11} = X_1$.

Building on this concept, we will now describe how to extend our method ([Algorithm 1](#)) for creating private noise mechanisms suitable for 2-dimensional range queries. Initially, we'll utilize [Algorithm 1](#) to sample the summation of all 2^{k_2} columns, meaning the noise values indexed as (\emptyset, J) . Following that, we will implement the aforementioned strategy to divide each of these column totals into smaller groups of $2, 4, 8, \dots, 2^{k_1}$ values. The detailed algorithm is described below.

Algorithm 3 Noise Allocation Mechanism for two-dimensional range queries

Input: Depths K_1, K_2 of the binary tree indexing rows and columns, variance σ^2 determined by the privacy budget.

Output: Noise values $\{X_{I,J}\}$ for all node pairs $(I, J) \in \cup_{0 \leq k_1 \leq K_1} \{0, 1\}^{k_1} \times \cup_{0 \leq k_2 \leq K_2} \{0, 1\}^{k_2}$

Fix $I = \emptyset$, implement [Algorithm 1](#) to assign $X_{\emptyset, J}$ for every $J \in \cup_{0 \leq k_2 \leq K_2} \{0, 1\}^{k_2}$

for each node $\star \in \{0, 1\}^{k_1}$ for some $0 \leq k_1 \leq K - 1$ **do**

 Implement [Algorithm 1](#) to assign $Y_{\star, J}$ for every $J \in \cup_{0 \leq k_2 \leq K_2} \{0, 1\}^{k_2}$

 Define the noise values for the children nodes of \star :

$X_{\star 0, J} := \frac{1}{2}X_{\star, J} + \frac{\sqrt{3}}{2}Y_{\star, J}$ for every J

$X_{\star 1, J} := \frac{1}{2}X_{\star, J} - \frac{\sqrt{3}}{2}Y_{\star, J}$ for every J

end for

It is not hard to verify from the construction that every $X_{I,J}$ has the same marginal distribution, and satisfies $X_{I,J} = X_{I0,J} + X_{I1,J}$ and $X_{I,J} = X_{I,J0} + X_{I,J1}$. The computational cost of [Algorithm 3](#) is also linear with the number of data points. More detailed analysis of the appropriate level for the privacy budget, along with an analysis of utility, will be deferred to our future research.

C Additional experiments

In this section, we demonstrate numerical experiments for when the workload matrix consists of node and random queries and also runtime comparisons.

C.1 Node queries

Consider a binary tree such that elements of \mathbf{x} form the leaves of the tree. The queries are the nodes (including leaves) of this tree, which correspond to an interval summing up the leaves of tree rooted at the particular node. The error values are shown in [Fig. 6](#).

The gap in utility across mechanisms for $\text{err}_{\mathbf{W},2}(\mathcal{W}_\sigma)$ is small with Wavelet and ours providing smallest error values, then closely followed by remaining mechanisms. But that is not the case for $\text{err}_{\mathbf{W},\infty}(\mathcal{W}_\sigma)$, where Gaussian and EigenDesign perform significantly worse. The remaining mechanisms perform very similarly (except for Binary Tree which has slightly larger error) as n increases. The gap in correlated input perturbation and Binary tree mechanism is easier to see which comes from the smaller constant for noise that is required for guaranteeing privacy ($2 + \frac{2}{3} \log n$ vs $\log n$).

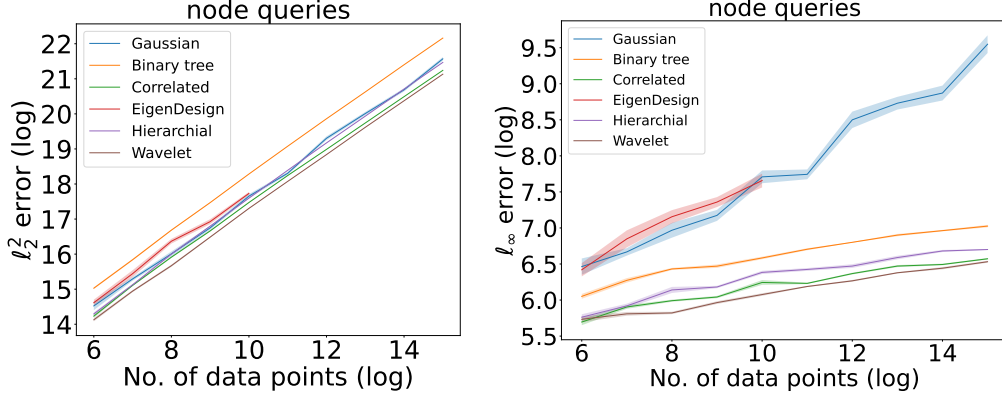


Figure 6: $\text{err}_{\mathbf{W},2}(\mathcal{W}_\sigma)$ and $\text{err}_{\mathbf{W},\infty}(\mathcal{W}_\sigma)$ for node queries.

C.2 Random queries

Here, each query asks for sum of random elements from \mathbf{x} . Note that unlike first two settings, the query is not contiguous over elements in \mathbf{x} . We sample the queries as follows - for each query we sample a number $k \in \{n/4, \dots, n\}$ (to simulate dense queries). We then sample k indices uniformly at random from $[n]$ and these indices form the query (these indices are set to 1 for the particular row in \mathbf{W}). We fix number of queries to be 2500. The results are shown in Fig. 7

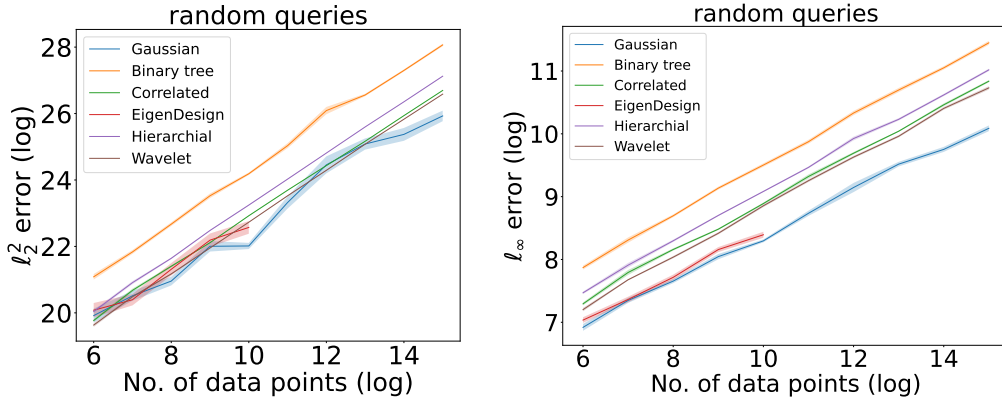


Figure 7: $\text{err}_{\mathbf{W},2}(\mathcal{W}_\sigma)$ and $\text{err}_{\mathbf{W},\infty}(\mathcal{W}_\sigma)$ for random queries.

For this setting of workload matrix, EigenDesign and Gaussian mechanism perform best utility wise for both $\text{err}_{\mathbf{W},2}(\mathcal{W}_\sigma)$ and $\text{err}_{\mathbf{W},\infty}(\mathcal{W}_\sigma)$. Wavelet, ours and Hierarchical perform almost similarly w.r.t noise magnitude whereas Binary tree mechanism has the largest noise. Hierarchical, ours and Binary tree mechanisms are more suited for sum over contiguous arrays by design, and as a result for random queries they perform worse. Gaussian mechanism has the least error majorly due to the fact that the noise scale is smallest due to smaller sensitivity. To see this, note that the queries sum over $O(n)$ elements in \mathbf{x} . For Gaussian, this corresponds to sum of $O(n)$ i.i.d Gaussians, whereas for Hierarchical and Correlated mechanism, worst case we still sum over $O(n)$ elements but with higher variance (by a factor of $O(\log n)$), resulting in larger noise added to the query answers.

C.3 Runtime comparison

We compare runtime for different mechanisms in seconds for answering the queries provided by the given workload matrix. For runtime, Gaussian and Wavelet are typically the fastest across different settings

of workload matrix and n whereas our mechanism is competitive with these and faster than Hierarchical. EigenDesign typically takes the longest which is expected as it involves eigencomposition of the matrix $\mathbf{W}^T \mathbf{W}$.

C.4 Implementation Details

We first describe the implementation for all mechanisms used in evaluations. All experiments were performed on a Macbook Pro with M1 processor and 16GB of RAM. Code is implemented in python language. **Binary Tree:** Here the mechanism builds a binary tree with elements being the leaves of the tree, and appropriately scaled Gaussian noise (for preserving privacy) is added to the the counts of nodes. We use the segment tree package for building and answering queries. **Hierarchical and Wavelet:** Hierarchical mechanism follows the same methodology as the Binary tree mechanism, followed by post-processing to find consistent sums for the internal nodes. We use the implementation from dpcomp-core package Hay et al. (2016) for Hierarchical and Wavelet. **EigenDesign:** We implement the mechanism using cvxopt for the optimization primitives. We use the cvxopt solver as in our experiments the default solver failed to converge for random queries and cvxopt converged to optimum faster. **Gaussian and Correlated mechanism:** Implementing these mechanisms is straight forward by adding appropriately scaled noise for privacy and then using the private histograms to answer queries.

Monte Carlo sampling for estimating errors of continuous queries: Now we discuss some implementation details of the continuous range queries in Section 4.2. After implementing the Cascade Sampling algorithm for the correlated perturbation $\mathcal{M}_\sigma(\mathbf{x}) = \mathbf{x} + \mathbb{N}(\mathbf{0}, \sigma^2 \mathbf{C}_k)$, calculating the error introduced by all the $\Theta(n^2)$ continuous range queries requires a cost of $O(n^3)$ to sum up all the noises in the corresponding entries, which is prohibitive when n is large.

Our primary goal is to evaluate the errors $\text{err}_{\mathbf{W},2}(\mathcal{W}_\sigma)$ and $\text{err}_{\mathbf{W},\infty}(\mathcal{W}_\sigma)$ in comparison to current algorithms, so we employ the Monte Carlo method for estimating these errors. It is clear from the mean and standard deviation plot presented in Fig. 4 that our estimation is sufficiently accurate.

We now outline the implementation process for $n \geq 2^8$. In each iteration, we uniformly select one range from all $\binom{n}{2} + n$ queries. This step is repeated m times. Using the m sampled errors E_1, \dots, E_m , we estimate $\text{err}_{\mathbf{W},2}(\mathcal{W}_\sigma)$ and $\text{err}_{\mathbf{W},\infty}(\mathcal{W}_\sigma)$. For instance, $(\binom{n}{2} + n) \times \sum_{i=1}^m (E_i^2) / m$ serves as an unbiased estimator for $\text{err}_{\mathbf{W},2}(\mathcal{W}_\sigma)$, becoming more accurate as m increases. Additionally, $\max_i E_i$ consistently estimates $\text{err}_{\mathbf{W},\infty}(\mathcal{W}_\sigma)$.

In further details, to uniformly select a continuous range, our sampling method involves: 1. Flip a coin with head probability $2/(n+1)$. 2. If heads, then random choose one element in $\{1, \dots, n\}$. 3. If tails, uniformly choose two distinct elements and use $\min\{n_1, n_2\}$ to $\max\{n_1, n_2\}$ as our range.

A final remark is that one could compute all $\binom{n}{2} + n$ errors without Monte Carlo methods using faster than $O(n^3)$ algorithms by properly storing intermediate results. However, these are not implemented in our current work.

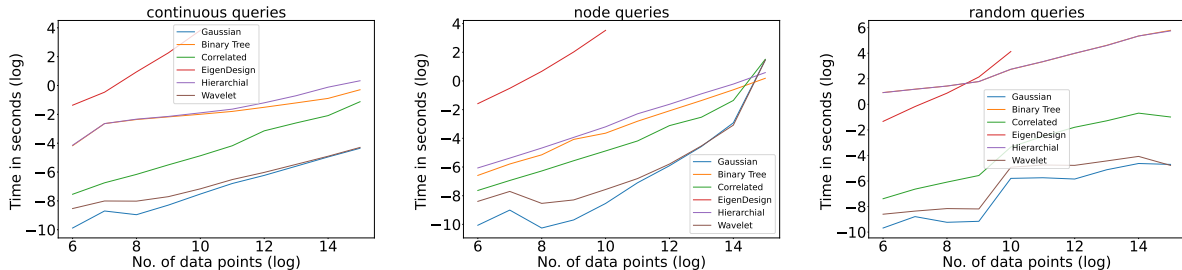


Figure 8: Runtime comparison for different configurations of the workload matrix.